

**Identification of palmitoyl substrate-enzyme pairs in neurons
through *in silico* proteomics**

Shinichiro Oku

DOCTOR OF PHILOSOPHY

Department of Physiological Sciences
School of Life Sciences
The Graduate University of Advanced Studies

2011

Acknowledgements

I gratefully acknowledge my research advisers Drs. Masaki Fukata and Yuko Fukata for all their support and advice for my PhD study. I thank my dissertation committee members, Drs. Ryuichi Shigemoto and Yoshihiro Kubo (National Institute for Physiological Sciences, Japan) and Mitsuharu Hattori (Nagoya City University, Japan), for spending their time on my dissertation and for their constructive comments.

I appreciate corporation with many scientists, Drs. Makoto Tominaga (National Institute for Physiological Sciences, Japan) and Ardem Patapoutia (The Scripps, CA) for TRPM8 plasmid, Akihiro Yamanaka (National Institute for Physiological Sciences, Japan) for orexin receptor plasmids, Yasuo Mori (Kyoto University, Japan) for TRPC1 plasmid, David Brecht (Johnson & Johnson, NJ) for TARP γ 2, TARP γ 8, and liprin- α 2 plasmids, Kozo Kaibuchi (Nagoya University, Japan) for zyxin and paxillin plasmids, Gary Banker (Oregon Health Science University, OR) for KIF5C plasmid, Ulli Bayer (University of Colorado, Denver, CO) for CaMKII α plasmid, Akihiko Kato (Eli Lilly, IN) for homer 1C plasmid, Xin-Ming Ma (University of Connecticut Health Science Center, CT) for kalirin7 plasmid, and Takao Hamakubo, Hiroko Iwanari and Yasuhiro Mochizuki (University of Tokyo, Japan) for DHHC1 and 10 antibodies.

I would like to thank people in the lab, Jun Noritake, Naoki Takahashi, Tsuyoshi Iwanaga, Norihiko Yokoi, Toshika Ohkawa, Yumi Suzuki, and Mie Watanabe for their help.

Lastly, to my family, thank you for always supporting me and believing in me.

Table of Contents

Table of Contents	4
Abbreviations	5 - 7
Summary	8 - 11
Introduction	12 - 16
Materials and Methods	17 - 35
Results	36 - 49
Discussion	50 - 56
References	57 - 65
Figure Legends	66 - 72
Tables	73 - 79
Figures	80 - 88

Abbreviations

2-ME	2-mercaptoethanol
aa	Amino acids
ABE method	Acyl-biotinyl exchange method
AMPA	2-amino-3-(5-methyl-3-oxo-1,2-oxazol-4-yl)propanoic acid
AMPAR	AMPA receptor
ATP	Adenosine-5'-triphosphate
Biotin-HPDP	N-[6-(Biotinamido)hexyl]-3'-(2'-pyridyldithio)propionamide
BSA	Bovine serum albumin
CaMKII α	Ca ²⁺ /calmodulin-dependent protein kinase II α
CBB	Coomassie brilliant blue
cDNA	Complementary DNA
CM	Chloroform methanol
CNIH2	Cornichon-2
CSS-Palm 2.0	Clustering and scoring strategy-Palm 2.0
C-terminus	Carboxyl-terminus
DHPG	Dihydroxyphenylglycine
DIV	Days in vitro
DMEM	Dulbecco's modified Eagle's minimal essential medium
DNA	Deoxyribonucleic acid

DTT	Dithiothreitol
EDTA	Ethylenediaminetetraacetic acid
<i>e.g.</i>	Exempli gratia
GABA _A R γ 2	Gamma-aminobutyric acid A receptor γ 2 subunit
GST	Glutathione S-transferase
HA	Hemagglutinin
HEK293	Human embryonic kidney 293
IAP	Immunoaffinity purification
<i>i.e.</i>	Id est
IPTG	Isopropyl β -D-1-thiogalactopyranoside
KD	Knockdown
KO	Knockout
LTD	Long-term depression
LTP	Long-term potentiation
mGluR	metabotropic glutamate receptor
miRNA; miR	Micro RNA
Ncdn	Neurochondrin
NEM	N-ethylmaleimide
NMDA	N-methyl-D-aspartic acid
N-terminus	Amino-terminus

OX2R	Orexin receptor type2
PAT	Palmitoyl acyl transferase
PBS	Phosphate buffered saline
PMSF	Phenylmethanesulfonylfluoride
PPT	Palmitoyl protein thioesterase
RNA	Ribonucleic acid
RT	Room temperature
RT-PCR	Reverse transcription-polymerase chain reaction
SDS-PAGE	Sodium dodecyl sulfate-polyacrylamide gel electrophoresis
TARPs	Transmembrane AMPA receptor regulatory proteins
TCEP	Tris(2-carboxyethyl)phosphine
TEV	Tobacco etch virus
TRP	Transient receptor potential
TRPC1	Transient receptor potential cation channel, canonical subfamily, member 1
TRPM8	Transient receptor potential cation channel, melastatin subfamily, member 8
Tris	Tris(hydroxymethyl)aminomethane
Vol.	Volume
WT	Wild type

Summary

Posttranslational modifications, including phosphorylation, ubiquitination, glycosylation and lipidation, provide proteins with additional regulatory systems beyond genomic information.

Protein palmitoylation is the most common reversible lipid modification and plays significant roles in protein trafficking and function. Palmitoylation modifies numerous classes of proteins including signaling proteins, synaptic scaffolding proteins, and various transmembrane proteins.

Identification of palmitoyl substrates is important for elucidating physiological roles of protein palmitoylation. Recently, a large family of 23 DHHC proteins has emerged as mammalian palmitoylating enzymes, and several enzyme-substrate pairs have begun to be reported. Also, the recent development of the palmitoyl-proteomic methods has identified a lot of novel substrates.

However, the conventional proteomic analysis depends on the biochemical property of the target proteins and thereby may omit important substrates to understand whole “palmitome.”

Here, to systematically identify novel palmitoyl substrates, I performed in silico whole-genome screening using CSS-Palm 2.0 program, which is a free software for palmitoylation site prediction. I lined up about 60,000 mouse protein sequences from UniProt database according to the CSS-Palm scores, and selected 17 candidates as novel palmitoyl substrates, which accumulate at the specific membrane domains like synaptic membranes, and cell-to-cell and cell-to-substratum junctions. Then, I experimentally verified their palmitoylation. I investigated by the metabolic labeling method whether these candidate proteins are actually palmitoylated by

a general palmitoylating enzyme, DHHC3, in HEK293 cells and found that DHHC3 palmitoylated 10 candidates. These proteins included: a presynaptic protein, Syd-1; postsynaptic proteins, transmembrane AMPA receptor regulatory proteins (TARP) γ 2, TARP γ 8, cornichon-2, CaMKII α and neurochondrin (Ncdn); a focal adhesion protein, zyxin; transient receptor potential (TRP) channels, M8 and C1; and G-protein coupled receptor, orexin receptor type2. Of these novel substrates, I selected four proteins, Syd-1, Ncdn, TARP γ 8 and CaMKII α , and confirmed that all tested endogenous proteins were palmitoylated in hippocampal neurons by the acyl-biotinyl exchange (ABE) method. By the subsequent screening of 23 DHHC proteins, I found that Ncdn was robustly palmitoylated by the DHHC1/10 subfamily, whose palmitoylating activity has not yet been reported, and the DHHC3/7 subfamily. Therefore, I focused on this novel substrate-enzyme pair, Ncdn and DHHC1/10. Ncdn is a neuron-specific cytosolic protein and regulates neurite-outgrowth and mGluR-related synaptic plasticity. Also, genetic evidence using the knockout mouse indicates that Ncdn associates with epileptic seizure and schizophrenia.

As predicted by CSS-Palm 2.0, Ncdn was palmitoylated at the amino-terminal cysteine residues (at positions 3 and 4), which were shared with both DHHC1/10 and DHHC3/7 subfamilies. DHHC3 palmitoylated many proteins including Ncdn as well as previously reported palmitoyl substrates, GluA2 and G α q, whereas DHHC10 palmitoylated only Ncdn. DHHC1/10 subfamily, but not DHHC3/7 subfamily, was co-purified with Ncdn from the brain lysate indicating the

physical interaction between DHHC1/10 subfamily members and Ncdn. Overexpression of DHHC1/10 subfamily specifically relocalized Ncdn near peri-nuclear structures in a palmitoylation-dependent manner in COS7 cells. Thus, DHHC3/7 subfamily and DHHC1/10 subfamily may differently recognize Ncdn as a palmitoyl substrate.

I found that Ncdn expression was increased during dendrite development in cultured neurons and that Ncdn protein was biochemically fractionated into both cytosolic and membrane fractions of the brain tissue. Ncdn was specifically localized at somato-dendritic regions in hippocampal neurons and partly co-localized with HA-tagged DHHC1/10 subfamily in dendritic shafts and dendritic spines. Palmitoylation-deficient mutant of Ncdn delocalized from dendritic membrane structures in hippocampal neurons. Furthermore, knockdown of DHHC1, but neither DHHC3 nor DHHC10, significantly reduced dendritic localization of Ncdn, indicating that DHHC1 is a physiological palmitoylating enzyme to regulate the specific Ncdn localization in neurons. Future functional studies on DHHC1-mediated Ncdn palmitoylation will clarify how this novel substrate-enzyme pair is involved in neuronal differentiation and functions such as dendrite development.

Finally, I systematically screened mouse whole-genome for palmitoyl-substrates through computational prediction (*in silico* proteomics), and found that Ncdn is the first substrate for the DHHC1/10 subfamily, and that DHHC1 plays a critical role in proper localization of Ncdn to

dendrites in neurons. Thus, this study indicates that in silico approach is useful for the discovery of novel palmitoyl substrates and complementally functions with previous experimental methods. Increased information of palmitoyl substrate-enzyme pairs will be the solid foundation for understanding molecular mechanisms and regulatory roles of protein palmitoylation in the dynamic cellular functions.

Introduction

Protein palmitoylation is the first discovered and the most common lipid modification. This modification, the attachment of the 16-carbon saturated fatty acid palmitate to one or more cysteine (Cys) residues by labile thioester linkage, increases hydrophobicity of proteins, promotes their membrane association with intracellular and plasma membranes, and regulates protein trafficking and function (1-3). Palmitoylation modifies numerous important proteins throughout the body including G-protein α subunits ($G\alpha_s$, $G\alpha_q$, $G\alpha_{i2}$), numerous G-protein coupled receptors (Rhodopsin, β 2-adrenergic receptor), small GTPases (H-Ras, RhoB, Cdc42), cell adhesion molecules (integrin α 6, NCAM, DCC, L1), ion channels (GluAs, GluN2A) and scaffolding proteins (PSD-95, GRIP, δ -catenin) (1, 3, 4). Unlike other lipid modification, such as myristoylation or prenylation, palmitoylation is a reversible reaction, which can be regulated by extracellular signals. The reversible nature of palmitoylation allows proteins to shuttle between intracellular compartments, relocalize in physiological contexts and participate in diverse aspects of cellular signaling (1-3).

The dynamic palmitoylation level is finely controlled by palmitoyl acyl transferases/palmitoylating enzymes (PATs) and palmitoyl protein thioesterases/depalmitoylating enzymes (PPTs). In 2002, forward genetic screening in yeast identified Erf2/4 (5, 6) and Akr1 (7) as PATs for yeast RAS2 and yeast casein kinase 2, respectively. Erf2 and Akr1 share the conserved Cys-rich DHHC (Asp-His-His-Cys) domain and four or six transmembrane domains,

respectively (**Figure 1A**). The DHHC sequence and its surrounding sequence are essential for their enzymatic activity. DHHC proteins are evolutionally conserved from yeast (7 kinds) (5, 7, 8) plants (9) to mammals (23 kinds) (**Figure 1B**) (10). Originally, some of mammalian DHHC proteins had been reported to be associated with human disorders (**Table 1**). Mutations of DHHC2 were found in colorectal cancers (11). DHHC8 was proposed as a candidate gene for schizophrenia (12-14), and DHHC9 and DHHC15 have been reported to be associated with X-linked mental retardation (15, 16). DHHC17 was identified as one of the huntingtin-interacting proteins (HIP14) (17). However, their biological functions had not been elucidated. In 2004, several groups including our laboratory revealed that some of mammalian DHHC proteins function as authentic PATs (10, 18, 19). Twenty-three DHHC proteins can be categorized into some subfamilies based on the homology of their catalytic DHHC domains (10). For example, DHHC2 and 15 belong to the same subfamily while DHHC3 and 7 form another subfamily (**Figure 1B**). The discovery of the mammalian PAT family and the establishment of the simple screening system using DHHC protein library have facilitated identification of a lot of palmitoyl substrate-enzyme pairs. Importantly, the same subfamily of DHHC proteins often shares its substrates. For example, DHHC3/7 subfamily palmitoylates most of palmitoyl-proteins, such as PSD-95 (4, 20-22), G α (23), SNAP-25 (23), NCAM-140 (24) and so on (**Figure 1B**). DHHC2/15 subfamily specifically palmitoylates PSD-95 (**Figure 1B**) (25). Also, DHHC9/18 subfamily palmitoylates H-Ras (**Figure 1B**) (10, 26). However, the identified number of the substrate-enzyme pair is still limited, and thereby enzymatic activities of some DHHC proteins,

such as DHHC1/10 subfamily, remain unknown because of no identification of their substrates. Thus, in this study, I aimed to identify novel palmitoyl substrate-enzyme pairs and pursued their physiological relevance.

To date, without knowing canonical consensus sequences for palmitoylation, palmitoyl substrates have been identified only by metabolic incorporation of radio-labeled palmitate followed by immunoprecipitation of each candidate protein (*e.g.*, GAP-43 (27), PSD-95 (28)).

This classical approach depends on the keen prediction based on the biochemical properties of the individual protein (*e.g.*, detergent insolubility from the membrane fraction) or the immunocytochemical analysis (*e.g.*, membrane localization of cytoplasmic proteins) and lacks any means of comprehensive profiling palmitoylated proteins. Recently, several groups developed a new proteomic method in which palmitoylated proteins are purified from cells or tissues and identified as palmitoyl substrates by combining with mass spectrometry. One purification method of palmitoylated proteins is called acyl-biotinyl exchange (ABE) method (4, 20-22), which consists of three steps: first, blockade of unmodified free cysteine thiols of proteins with N-ethylmaleimide; second, specific cleavage of palmitoylation thioester linkages from palmitoylated cysteines with hydroxylamine; and third, labeling of newly exposed cysteinyl thiols with a thiol-specific biotinylaiton reagent. The biotinylated proteins are purified with streptavidin beads. As another method, click chemistry is applied for the purification (29, 30).

Substrate proteins are metabolically labeled with (non-radiolabeled) palmitic acid analog and

reacted with biotin-azides as bioorthogonal chemical reporter. Biotin-labeled proteins are then purified with streptavidin beads. In both methods, purified samples are analyzed by mass spectrometry to identify palmitoyl substrates. Although these powerful proteomic analyses have identified many new palmitoyl-proteins (4, 21, 29), this method using mass spectrometry possesses several potential problems. First, some proteins are expressed at too low in cells or tissues to be identified by mass spectrometry. Second, some of the membrane proteins, such as G-protein couple receptors or ion channels, are barely extracted from cells by detergent, failing to be purified (31, 32). Third, protein modifications including phosphorylation, palmitoylation and so on may prevent identification by mass spectrometry (33). Furthermore, some proteins that are not palmitoylated but interacted and co-purified with palmitoylated proteins might be contaminated (false positive results). Lastly, it is very time consuming to identify palmitoylation sites by mass spectrometry (34). Our method in this study, *in silico* predictions of palmitoylation sites of proteins is profitable to complementally overcome those problems and identify novel palmitoyl substrates.

Here, I found that neurochondrin (Ncdn)/Norbin is one of the novel palmitoyl substrates. Ncdn was originally identified as a gene whose expression is upregulated when long-term potentiation (LTP) is chemically induced with tetraethylammonium, a potassium channel blocker (35). Ncdn is a 75-kDa neuronal cytoplasmic protein and does not have any obvious domain structures and functional motifs (36). Shiozaki *et al.* reported that overexpression of Ncdn in Neuro2A cells

promotes neurite-outgrowth (35). Knockout (KO) mouse of *Ncdn* leads to early embryonic lethal between 3.5 and 6.5 days post coitus (37). Nervous system-specific conditional KO mouse shows epileptic seizure (38). Forebrain-specific *Ncdn* KO mouse attenuates mGluR5-dependent stable change in synaptic transmission in the hippocampus and shows a behavioral phenotype associated with a rodent model of schizophrenia (39). This study also showed that *Ncdn* regulates surface expression of mGluR5 (39). Furthermore, *Ncdn* was reported to interact with various proteins, such as Sema4C (40), several G-protein coupled receptors (39, 41, 42), and *Dial1* (43), an actin nucleation factor (44). Taken together, *Ncdn* is suggested to be a promising central nervous system regulator and functions as a scaffolding protein or an adaptor protein. However, its precise subcellular localization in neurons and regulatory mechanism remain unclear.

In this study, I systematically screened mouse whole-genome for palmitoyl-substrates through computational prediction (*in silico* proteomics). I identified at least 10 novel palmitoyl-substrates including *Ncdn*. I found that DHHC1/10 subfamily and DHHC3/7 subfamily quantitatively palmitoylated *Ncdn* at Cys-3 and Cys-4. This finding for the first time demonstrates that DHHC1 and DHHC10 are functional palmitoylating enzymes. *Ncdn* and DHHC1/10 subfamily were co-localized in dendritic shafts and dendritic spines. DHHC1, but not DHHC3 and 10, knockdown significantly reduced the amount of dendritic *Ncdn*. Thus, *Ncdn* palmitoylation by DHHC1/10 subfamily plays a critical role in its dendritic membrane localization in neurons.

Materials and Methods

Genome-wide *in silico* prediction of palmitoylated proteins

For the genome-wide prediction of palmitoyl proteins with their sites, I used an updated software, CSS-Palm 2.0—Palmitoylation Site Prediction using a Clustering and Scoring Strategy (<http://csspalm.biocuckoo.org/prediction.php>) (45). This software algorithm is based on experimentally verified palmitoylation sites: 263 palmitoylation sites from 109 distinct palmitoyl proteins, manually collected from scientific literatures and clustered into three clusters, including Type I (sites follow a –CC– pattern, C is a cysteine residue), Type II (sites follow a –CXXC– pattern, X is a random residue), and Type III (other sites) groups (45).

The mouse proteome sequence data consisting of redundant 62,695 sequences was downloaded from UniProt database (<http://www.uniprot.org/>). Sequence files were saved as separate text files in FASTA format programmed by Perl and used as the input of the locally installed CSS-Palm 2.0 (without setting threshold). To run automatically CSS-Palm 2.0 for all sequence files, the condition used was Windows XP Professional SP3 32 bit, UWSC Ver4.6c, and Java Access Bridge for Microsoft Windows Operating System Ver.2.0.1. The output CSV file included results with positions of predicted palmitoyl cysteines, the surrounding sequence and CSS-Palm Scores for each protein. All the datasets from CSS-Palm 2.0 included 59,157 files of proteins which have any cysteine residues. Protein files only with score ‘zero’ cysteines were then removed. The resultant 59,136 proteins (with score>0) were listed-up in order of scores in CSV file format

(available at <http://www.nips.ac.jp/fukata/palm2/>), which included ~19,000 proteins with the score greater than cutoff score of 1.8. Redundant sequences and sequences with cysteines in signal sequences were further removed.

To find palmitoyl-candidate proteins that are expressed predominantly in brain tissue, the listed protein sequences above were further analyzed by a gene expression database, BodyMap-Xs (<http://bodymap.jp>). The entire datasets for mouse genes (38,632 gene data) were automatically downloaded from BodyMap-Xs at the following conditions; Windows XP Professional SP3 32bit, Strawberry Perl for Windows Ver.5.12.3.0, the structure of Perl module is as follows; LWP::UserAgent, HTML::Entities; HTML::TreeBuilder::XPath; HTML::Selector::XPath gw/selector_to_xpath/; Text::CSV_XS. Perl module was used for the composition of the table written in HTML and data files were saved as CSV files. The information about accession numbers (Unigene#) included in each output data file from BodyMap-Xs was collated with the UniProt annotation in the initial output data files from CSS-Palm 2.0. Then the CSS-Palm-predicted candidates included in datasets from BodyMap-Xs analysis were further extracted. The brain enrichment score was calculated by dividing the score for brain by the sum of scores for all tissues. The table was made with UniProt accession number, CSS-Palm score, and BodyMap-Xs accession number (Unigene#) and brain enrichment score, ranked in order of the CSS-Palm score. Because the present expression database is not sufficient for all the proteins, this narrow-down process may omit 27% of CSS-Palm 2.0 data that is not covered in the

BodyMap-Xs database.

I noted that the resultant list consisting of ~750 candidates includes many proteins with high CSS-Palm scores, which are known to be enriched in specific membrane domains such as pre- and postsynapses and cell adhesions (tight and adherens junctions). Thereby, I re-inspected the initial list from CSS-Palm 2.0 before BodyMap-Xs data was collated, and also selected postsynaptic proteins, kalirin7 and homer 1C, presynaptic proteins, Syd-1, motor protein, KIF5C, focal adhesion proteins, paxillin and zyxin; and a tight junction protein, Par3, as additional palmitoyl candidates (Score > 1.8).

Cloning and plasmid constructions

Reverse transcription-polymerase chain reaction (RT-PCR)

Some substrate candidate cDNAs were obtained by RT-PCR (**Table 2**). To prepare rat brain total RNA, rat whole brain was homogenized with Trizol (Invitrogen). The homogenate was mixed with chloroform and stood for 2 minutes at room temperature (RT), followed by centrifugation at 11,000 x g at 4°C for 15 minutes. The supernatant was mixed with isopropanol and stood for 10 minutes at RT, followed by centrifugation at 11,000 x g at 4°C for 10 minutes. The supernatant was removed and the pellet was rinsed with 75% ethanol, followed by centrifugation at 7,200 x g at 4°C for 5 minutes. After the supernatant was removed, the pellet of total RNA was dried at RT and dissolved in RNase-free water. 2 µg of total RNA was used for first-strand cDNA synthesis

with Superscript-III reverse transcriptase system (Invitrogen) according to the manufacture protocol. Then, cornichon-2 (CNIH2), neurochondrin (Ncdn), Rab3A, Syd-1 and Par3 cDNAs were amplified by PCR with KOD-plus-DNA polymerase (TOYOBO) with specific primer sets (see **Table 2**). PCR cycling parameters were one cycle of 5 minutes at 98°C and 30 cycles of 30 seconds at 98°C, 30 seconds at 52°C and 5 minutes at 68°C.

Subcloning

cDNAs of liprin- α 2, kalirin7, CaMKII α , transient receptor potential channel melastatin (TRPM)8, TARP γ 2, TARP γ 8, homer 1C, transient receptor potential channel canonical (TRPC)1, orexin receptor type2 (OX2R), paxillin, zyxin and KIF5C were kindly provided. The primer sets used for subcloning, clone IDs and providers were listed in **Table 2**. The following constructs were generated by PCR and all constructs were confirmed by DNA sequencing analysis.

CNIH2-GFP The cDNA was inserted into pEGFP-N2 at the EcoRI site to fuse GFP at the carboxyl (C)-terminus.

Ncdn For figure 4F, the cDNA was inserted into pEGFP-C2 at the EcoRI site or pEGFP-N2 at the EcoRI to fuse GFP at the amino (N)- or C-terminus, respectively. For other experiments to express Ncdn-GFP, the cDNA of Ncdn was amplified from pEGFP-C2:NcdnWT by PCR using the primers 5'-GCTAGAATTCGCCACCATGTCGTGTTGTGACCTGGC-3' and

5'-GCTAGCGGCCGCGGGGCTCTGACAGGCACTGCTCCA-3'. The cDNA containing the EcoRI and NotI sites was inserted into pCAGGS-GFP(N). pCAGGS-GFP(N): Ncdn C3S, Ncdn C4S, Ncdn C3,4S were constructed by site-directed mutagenesis using the primers 5'-GCTAGAATTCGCCACCATGTCGTCTTGTGACCTGGCTGCGGCGGGAC-3' and 5'-GCTAGCGGCCGCGGGGCTCTGACAGGCACTGCTCCA-3', the primers 5'-GCTAGAATTCGCCACCATGTCGTGTTCTGACCTGGCTGCGGCGGGACAG-3' and 5'-GCTAGCGGCCGCGGGGCTCTGACAGGCACTGCTCCA-3', and the primers 5'-GCTAGAATTCGCCACCATGTCGTCTTCTGACCTGGCTGCGGCGGGACAG-3' and 5'-GCTAGCGGCCGCGGGGCTCTGACAGGCACTGCTCCA-3', respectively. To construct pCAGGS:Ncdn-HA, the cDNA of Ncdn was amplified from pCAGGS-GFP(N):NcdnWT by PCR using the primers 5'-GCTAGAATTCGCCACCATGTCGTGTTGTGACCTGGCTGCG-3' and 5'-GCTAGAATTCTCAAGCGTAATCTGGAACATCGTATGGGTAGGGCTCTGACAGGCAC TGCTCCA-3'. For the antigen production of Ncdn antibody (N-rNcdn), the cDNA encoding aa 1-59 was amplified by PCR from pEGFP-C2:NcdnWT using the primers 5'-GCTAGAATTCATGTCGTGTTGTGACCTGGCTGCG-3' and 5'-GCTAGAATTCTCATAGCAGCAGGGCTGCAAAGCTGCT-3' and subcloned into pET32H at the EcoRI site. To construct the expression vector of the GFP-fused Ncdn N-terminal peptides, sense oligonucleotides and antisense oligonucleotides were phosphorylated in the mixture (Protruding end kinase buffer (TOYOBO), 0.1 mM ATP, 1 μ M nucleotides, T4 polynucleotide

kinase) separately at 37°C for 30 minutes, then sense and antisense oligonucleotides were annealed. Resultant double-strand oligonucleotides were inserted into pEGFP-N2 at the BamHI and EcoRI sites.

GFP-Rab3A The cDNA was inserted into pEGFP-C2 at the EcoRI site.

GFP-Syd-1 The cDNA was inserted into pEGFP-C2 at the EcoRI site.

Par3(281; aa 1-281)-GFP The cDNA was inserted into pEGFP-N2 at the EcoRI site.

Liprin-α2 The cDNA was inserted into pCAGGS at the EcoRI site.

CaMKIIα-GFP The cDNA was inserted into pCAGGS-GFP(N) at the EcoRI and NotI sites.

TRPM8-Flag The cDNA was inserted into pCAGGS at the EcoRI site.

Expression vectors of HA-TARP γ2, TARP γ8, kalirin7-GFP, GFP-homer 1C, KIF5C (560; aa 1-560)-YFP, Flag-TRPC1, OX2R-GFP, GFP-paxillin and GFP-Zyxin were kindly provided (listed in Table 2).

pCAGGS-GFP(N):Gαq (23) and pcDNA3.1(+):CBP-Flag-GluR2 (46) were described previously.

pEF-Bos:HA-DHHC clones were described previously (10). To construct pcDNA3.1:Hisx6-TEV-Flag-mDHHC10, the cDNA of mouse DHHC10 was amplified from pEF-Bos:HA-mouse DHHC10 (mDHHC10) by PCR using the primers 5'-GCTACTCGAGATGAAAGAGATGAACATCTGTGG-3' and 5'-GCTACTCGAGCTAGTCTTCACTGTGGCAGATCT-3'. The cDNA was inserted into pcDNA3.1:Hisx6-TEV-Flag at the XhoI site. cDNAs of mouse DHHC2 and DHHC3 were

subcloned into pcDNA3.1:Hisx6-TEV-Flag as described previously (47).

To construct the knockdown vectors expressing microRNAs (miRNAs), BLOCK-iT RNAi Designer (Invitrogen) was used to select the targeting sequences, and the following targeting sequences were used (targeting both rat and mouse sequences): miR-Ncdn803, 5'-TCCTAGGAAGCAAGTTGAGCT-3'; miR-DHHC1_532, 5'-CACAGTGTGGCATCTGCTTTA-3'; miR-DHHC3_735, 5'-TGAGACGGGAATAGAACAATT-3'; miR-DHHC10_171, 5'-TGTCACCTTTGGGATCTTCAT-3' and miR-LacZ, 5'-GACTACACAAATCAGCGATTT-3' (as a negative control). These oligonucleotides were subcloned into pcDNA6.2:EmGFP-miR (Invitrogen). These miRNA sequences with EmGFP were amplified by PCR using the primers 5'-GATCGAATTCCAAGTTTGTACAAAAAAGCAGGC-3' and 5'-GATCGCGGCCGCGGCCCTCTAGATCAACCACTTTG-3' and subcloned into pCAGGS at the EcoRI and NotI sites.

Antibodies

The antibodies used are the following: rabbit polyclonal antibodies to TARP γ 2 and γ 8 (Millipore 07-577), Syd-1 (Abcam ab80402) and mGluR5 (Millipore 06-451); mouse monoclonal antibodies to Flag (Clone M2; Sigma F3165), CaMKII (Clone 6G9; Millipore MAB3119), PSD-95 (Clone 7E3-1B8; Thermo Fisher Scientific MA1-04), MAP2 (Clone HM-2; Sigma

M4403), pan-axonal neurofilament (Clone SMI312; Covance SMI312R), and synaptophysin (Clone SVP-38; Sigma S5768); rat monoclonal antibody to HA (Clone 3F10; Roche 12158167001) and chicken polyclonal antibody to GFP (Millipore ab16901). Rabbit polyclonal antibodies to GFP and moesin were described previously (47). Rabbit polyclonal antibody to Ncdn was raised against Hisx6-N-rat Ncdn (rNcdn) (aa 1 - 59) and affinity purified as described below.

Generation of anti-Ncdn antibody

To generate the antigen for Ncdn antibody, BL21 DE3 transformed with pET32H:N-rNcdn (aa 1 - 59) was grown in 2L Luria-Bertani culture with ampicillin until OD600 ~0.8-1.0. Expression of Hisx6-tagged N-rNcdn was induced with 0.1 mM IPTG for 4 hours at 25°C. BL21 DE3 was harvested at 5,100 x g at 4°C for 15 minutes. The pellet was suspended with ice-cold PBS and centrifuged at 5,100 x g at 4°C for 20 minutes. The cells were lysed with lysis buffer (10 mM imidazole, 300 mM NaCl, 20 mM Tris/Cl at pH 8.0, 10 µg/ml leupeptin, 50 µg/ml PMSF) and ultrasonicated for 30 seconds eight times, followed by centrifugation at 20,000 x g at 4°C for 1 hour. The supernatant was filtered through a 0.45 µm filter. The filtered supernatant was applied to a Ni-NTA agarose (Qiagen) column. The column was washed with wash buffer (20 mM imidazole, 300 mM NaCl, 20 mM Tris/Cl at pH 8.0). Hisx6-N-rNcdn was then eluted with E-buffer (250 mM imidazole, 300 mM NaCl, 20 mM Tris/Cl at pH 8.0) and dialyzed against PBS for immunization.

Rabbit polyclonal Ncdn antiserum, N-rNcdn, was raised (Operon Biotechnologies) and purified by the following procedure. Hisx6-N-rNcdn (for an antigen column) and another Hisx6-tagged fusion protein (for a dummy column) were coupled with cyanogen bromide beads (GE Healthcare) in coupling buffer (0.1 M NaHCO₃ at pH 8.3, 0.5 M NaCl,) overnight at 4°C. The coupled beads were centrifuged at 185 x g at RT for 5 minutes, and the supernatant was removed. The beads were mixed with blocking buffer (0.1 M Tris/Cl at pH 8.0, 500 mM NaCl) for 2 hours at RT, followed by centrifugation at 185 x g at RT for 5 minutes. The supernatant was removed, and the beads were packed in a column and washed with buffer 1 (50 mM Tris/Cl at pH 7.5) three times, coupling buffer three times, buffer 1, buffer 2 (50 mM Tris/Cl at pH 7.5, 0.5 M NaCl), elution buffer pH 2.5 (0.1 M glycine) and buffer 1. Antiserum was first applied to the dummy column to reduce antibodies to Hisx6 tag. The collected flow-through was applied to the antigen column. After washing the column with buffer 2 and buffer 1, the antibody was eluted with elution buffer pH 3.5 and then elution buffer pH 2.5. Concentration of purified IgG was estimated by Coomassie brilliant blue (CBB) staining.

Cell culture

HEK293 cells or COS7 cells were grown in DMEM supplemented with 10% fetal bovine serum (Sigma) at 37°C with 5% CO₂. Hippocampal and cortical neuron cultures were prepared from rat embryonic day 18–19 embryos. All animal experiments described herein were reviewed and

approved by the ethical committee in our institutes and were performed according to the institutional guidelines concerning the care and handling of experimental animals. Neurons were seeded as indicated in neurobasal medium (Invitrogen) supplemented with B-27 supplement (Invitrogen) and 2 mM Glutamax (Invitrogen).

Cell and brain lysate preparation

HEK293 cells/rat hippocampal and cortical neurons HEK293 cells (5×10^5 cells/6-well dish), rat hippocampal neurons at 33 DIV (5×10^5 cells/6-well dish) and rat cortical neurons at 30 DIV (5×10^5 cells/6-well dish) were lysed with SDS-PAGE sample buffer (62.5mM Tris/Cl at pH 6.8, 10% glycerol, 2% SDS, and 0.001% bromophenol blue) with 2-ME and boiled at 100°C for 5 minutes. The samples were subjected to SDS-PAGE and Western blotting with the indicated antibodies.

Rat brain P2 fraction/mouse whole brain homogenate Whole brain was homogenized in homogenizing buffer (20 mM Tris/Cl, 2 mM EDTA, 0.32 M sucrose, 100 µg/ml PMSF). 50 µg of the homogenate was analyzed by Western blotting with anti-Ncdn antibody. For preparation of P2 fraction, homogenate was centrifuged at 20,000 x g at 4°C for 1 hour. 50 µg of proteins was analyzed by Western blotting with anti-Ncdn antibody.

Metabolic labeling assay

HEK293 cells were seeded in 12-well plate (2.5×10^5 cells/well) and co-transfected with

HA-DHHC proteins, along with an individual substrate by Lipofectamine Plus reagent (Invitrogen). Twenty-four hours after transfection, HEK293 cells were preincubated for 30 minutes in serum-free DMEM with fatty acid-free bovine serum albumin (5 mg/ml; Sigma) and then labeled with 0.2 mCi/ml [³H]palmitic acid (PerkinElmer) for 4 hours in the preincubation medium. Cells were washed with PBS, scraped with SDS-PAGE sample buffer (62.5mM Tris/Cl at pH 6.8, 10% glycerol, 2% SDS, and 0.001% bromophenol blue) with 10 mM DTT and boiled at 90°C for 2 minutes. The labeled proteins were separated by SDS-PAGE. The gel was fixed with the fixation buffer (25% isopropanol and 10% acetic acid), and then the signals were amplified with the amplification buffer (1 M sodium salicylate, 15% ethanol). The dried gel was exposed to a film at -80°C for 3-7 days.

Acyl-biotinyl exchange (ABE) method

The ABE method was performed as previously described (4, 21, 22, 47). Hippocampal neurons (5 x 10⁵ cells/6-well dish) at 18-28 DIV were washed with PBS containing 10 mM N-ethylmaleimide (NEM) twice and solubilized with 0.1 ml of LB (50 mM Tris/Cl at pH 7.5, 5 mM EDTA, and 50 mM NaCl) containing 2% SDS and 10 mM NEM. After 15 minutes of extraction, LB with 2% Triton X-100 and 10 mM NEM was added to a final volume of 1 ml and incubated for 1 hour at 4°C. After centrifugation at 20,000 x g for 10 minutes, the supernatants were precipitated by the chloroform-methanol (CM) method. Precipitated protein was solubilized in 0.2 ml SB (50 mM Tris/Cl at pH 7.5, 5 mM EDTA, and 4% SDS) containing 10

mM NEM at 37°C for 10 minutes. The protein was diluted into 0.8 ml LB with 0.2% Triton X-100 and 1 mM NEM and incubated overnight at 4°C. NEM was removed by three sequential CM precipitations. Precipitated protein was solubilized in 0.2 ml of buffer SB, and then 0.8 ml HB (1 M hydroxylamine (NH₂OH) at pH 7.5, 150 mM NaCl, 0.2% Triton X-100, and 1 mM biotin-HPDP) or buffer TB (1 M Tris/Cl at pH 7.5, 150 mM NaCl, 0.2% Triton X-100, and 1 mM biotin-HPDP) was added. The mixture was incubated for 1 hour at RT and subjected to CM precipitation. The precipitated protein was dissolved in 0.2 ml SB, diluted into 0.8 ml LB containing 150 mM NaCl, 0.2% Triton X-100, and 200 μM biotin-HPDP, and incubated for 1 hour at RT. Free biotin-HPDP was removed by CM precipitation. The precipitated protein was solubilized in 100 μl of buffer UB (50 mM Tris/Cl at pH 7.5, 5 mM EDTA, and 2% SDS) and diluted in 900 μl LB with 0.2% Triton X-100. After brief centrifugation, the supernatant was incubated with 30 μl NeutrAvidin-agarose (Thermo Fisher Scientific 29200) for 1 hour at 4°C. After washing the beads with LB containing 0.1% SDS and 0.2% Triton X-100, bound proteins were suspended in SDS-PAGE sample buffer (62.5 mM Tris/Cl at pH 6.8, 10% glycerol, 2% SDS, and 0.001% bromophenol blue) with 2-mercaptoethanol (2-ME) at 100°C for 5 minutes. The samples were subjected to SDS-PAGE and Western blotting with the indicated antibodies.

For Ncdn palmitoylation, the improved ABE protocol (48) was used to reduce background signals. Here, to extract more proteins, LB included 4% SDS. Also, to cleave disulfide bonds prior to alkylation with NEM, tris(2-carboxyethyl)phosphine (TCEP), a potent reducing agent

that does not cleave thioester bond between palmitate and cysteine residue, was used. Briefly, cortical neurons (5×10^5 cells/6-well dish) at ~30 DIV were washed with PBS twice and solubilized with 0.25 ml SB (50 mM Tris/Cl at pH 7.5, 5 mM EDTA, 4% SDS) for 10 minutes at 37°C and then, LB (50 mM Tris/Cl at pH 7.5, 5 mM EDTA, 150 mM NaCl) containing 0.2% TritonX-100 was added to a final volume of 0.9 ml. After centrifugation at 20,000 x g at RT for 10 minutes, the supernatant was reduced with 0.1 ml of 100 mM TCEP (10 mM) in LB with 2% Triton-X 100 for 30 minutes at RT and then alkylated with 0.1 ml of 300 mM NEM (30 mM) for 2.5 hours at RT. The solutions were precipitated by CM method five times and the pellets were dissolved in SB and treated with 0.2% TritonX-100/1 mM biotin-HPDP containing 1 M NH₂OH or 50 mM Tris/Cl for 1 hour at RT. The solutions were precipitated by the CM method three times. The pellets were dissolved in 0.050 ml TB (50 mM Tris/Cl, 5 mM EDTA, 2% SDS) at 37°C for 10 minutes, diluted with 0.95 ml 0.2% TritonX-100/LB and centrifuged at 20,000 x g at RT for 5 minutes. The supernatants were incubated with NeutrAvidin agarose in 0.2% TritonX-100/LB containing 0.1% SDS for 1 hour at RT. After washing the beads with 0.2% TritonX-100/LB containing 0.1% SDS, bound proteins were processed as described above.

Subcellular fractionation

The method was basically followed as described previously (47, 49). In brief, five rat adult brains were homogenized in buffer containing 320 mM sucrose and 10 mM HEPES-NaOH, pH 7.4 (containing 0.2 mM PMSF). Homogenate was centrifuged for 10 minutes at 1,000 x g to

remove crude nuclear fraction (P1). The supernatant (S1) was centrifuged at 9,000 x g for 15 minutes to produce a pellet (P2) and supernatant (S2). The S2 was centrifuged at 100,000 x g for 1 hour to produce a pellet (P3; microsomal fraction) and supernatant (S3). The P2 fraction was resuspended in the homogenization buffer. Discontinuous sucrose gradients containing 3 ml of the resuspended P2 material and 3 ml each of 0.8, 1.0, and 1.2 M sucrose solutions in 10 mM Hepes-NaOH, pH 7.4, were run for 2 hours at 58,000 x g (SW41 rotor; Beckman Coulter). The band between 1.0 and 1.2 M sucrose was obtained as a synaptosome fraction (Syn). This synaptosome fraction was extracted with ice-cold 0.5% Triton X-100 in 0.16 M sucrose and 6 mM Tris/Cl, pH 8.1, and then centrifuged at 32,800 x g for 20 minutes to divide into soluble (Sol1) and insoluble fractions (PSD-1). The pellet was resuspended in 0.5% Triton X-100, 0.16 M sucrose, and 6 mM Tris/Cl, pH 8.1, and centrifuged at 200,000 x g for 1 hour to produce a pellet (PSD-2). 50 µg of proteins of each fraction was analyzed by Western blotting with the indicated antibodies.

Tandem-affinity purification

HEK293 cells transfected with Hisx6-Flag-DHHC2, 3 or 10 on a 10-cm dish were washed with PBS twice at RT. Cells were scraped with 0.75 ml IP buffer (20 mM Tris/Cl at pH 7.5, 1 mM EDTA, 100 mM NaCl, 2.0% TritonX-100, 50 µg/ml PMSF) and homogenized in a Potter-type homogenizer, followed by centrifugation at 100,000 x g at 4°C for 30 minutes. P2 membrane fraction was prepared by homogenization of rat whole brain in homogenizing buffer (20 mM

Tris/Cl, 2 mM EDTA, 0.32 M sucrose, 100 μ g/ml PMSF) and centrifugation at 20,000 x g at 4°C for 1 hour. The resultant pellet was suspended and homogenized with the HEK293 cell lysate prepared above. After extraction for 1 hour at 4°C, the homogenate was centrifuged at 100,000 x g at 4°C for 1 hour. The supernatant was incubated with Flag-M2 beads (Sigma) for 2 hours at 4°C. The beads were washed with IAP buffer (20 mM Tris/Cl, 150 mM NaCl, 1% TritonX-100) five times. Hisx6-Flag-DHHC was eluted with Flag peptide (0.25 mg/ml) for 1 hour at 4°C. The Flag eluate was incubated with Ni-NTA agarose for 1 hour at 4°C. The Ni-NTA agarose were washed with IAP buffer containing 20 mM imidazole four times. Hisx6-Flag-DHHC was eluted with IAP buffer containing 250 mM imidazole. The imidazole eluate was boiled in SDS-PAGE sample buffer at 100°C for 5 minutes. The samples were subjected to SDS-PAGE and Western blotting with the indicated antibodies.

Transfection and immunofluorescence analysis

Localization of HA-DHHCs

Hippocampal neurons (5×10^4 cells) on 12-mm coverslips were transfected with HA-DHHC1, 2, 3, 5, 7, 8, 10 or 15 at ~7 DIV by Lipofectamine 2000. Twelve days after transfection, neurons were fixed with methanol at -30°C for 10 minutes. Neurons were washed with ice-cold PBS for 10 minutes and then washed with 1 M Tris/Cl at pH 7.5 for 20 minutes on ice. Neurons were washed with ice-cold PBS, blocked with 10 mg/ml BSA for 10 minutes on ice, and then stained with rabbit polyclonal anti-Ncdn (1:100), rat monoclonal anti-HA (1:500) and mouse

monoclonal anti-PSD-95 (1:250) for 1 hour. Neurons were then stained with Alexa Fluor 488 goat anti-rabbit IgG (Invitrogen A11034), Cy3 donkey anti-rat IgG (Jackson ImmunoResearch), and Alexa Fluor 647 goat anti-mouse IgG (Invitrogen A21236) for 1 hour. Fluorescent images were obtained using an LSM5 Exciter system (Carl Zeiss) with a Plan-Apochromat 63X objective.

Knockdown of Ncdn

Cortical neurons (5×10^4 cells) at ~7 DIV were transfected with pCAGGS:EmGFP-miR-Ncdn803 by Lipofectamine 2000 (Invitrogen). Seven days after transfection, neurons were fixed with 4% paraformaldehyde/120 mM sucrose/100 mM HEPES at pH 7.4 at RT for 10 minutes, permeabilized with 0.1% Triton X-100 for 10 minutes on ice, and blocked with PBS containing 10 mg/ml BSA for 10 minutes on ice. Neurons were then labeled with rabbit polyclonal anti-Ncdn (1:100) and Cy3-conjugated donkey anti-rabbit IgG (Jackson ImmunoResearch). Knocked-down neurons were visualized with GFP.

Localization of Ncdn in neurons

Hippocampal neurons at ~40 DIV were fixed with methanol at -30°C for 10 minutes. Neurons were stained with rabbit polyclonal anti-Ncdn (1:100), together with mouse monoclonal anti-MAP2 (1:50), mouse monoclonal anti-pan-axonal neurofilament (1:5000), mouse monoclonal anti-synaptophysin (1:2000) or mouse monoclonal anti-PSD-95 (1:250) as the

primary antibodies, and Alexa Fluor 488 goat anti-rabbit IgG (Invitrogen A11034) and Cy3-conjugated donkey anti-mouse IgG (Jackson ImmunoResearch) as the secondary antibodies.

To examine whether DHHC3 or 10 is co-localized with Ncdn in neurons, hippocampal neurons were transfected with HA-DHHC3 or 10 at ~7 DIV by Lipofectamine 2000. Around two weeks after transfection neurons were fixed with methanol as described above and stained with rabbit polyclonal anti-Ncdn, rat monoclonal anti-HA and mouse monoclonal anti-PSD-95 as the primary antibodies, and then incubated with Alexa Fluor 488 goat anti-rabbit IgG (Invitrogen A11034), Cy3-conjugated donkey anti-rat IgG (Jackson ImmunoResearch), and Alexa Fluor 647 goat anti-mouse IgG (Invitrogen A21236).

Live imaging of GFP-fused Ncdn WT and palmitoylation-deficient mutant (Ncdn C3,4S) in COS7 cells

COS7 cells were seeded onto a poly-D-lysine-coated 35-mm glass-bottom dish (Iwaki) and co-transfected with Ncdn WT-GFP or Ncdn C3,4S-GFP, along with HA-DHHC3 or 10. Eight hours after transfection, COS7 cells were observed at 37°C in a CO₂ chamber (Tokai Hit) using an LSM5 Exciter system (Carl Zeiss) with a Plan-Apochromat 63X objective.

Localization of Ncdn WT and Ncdn C3,4S in neurons

Hippocampal neurons were transfected with Ncdn WT-GFP or Ncdn C3,4S-GFP at ~7 DIV by

Lipofectamine 2000. Neurons were fixed with methanol at ~30 DIV and immunostained with chicken polyclonal anti-GFP (1:250) and Alexa Fluor 488 goat anti-chicken IgG (Invitrogen A11039). For extraction of neurons with 0.1% TritonX-100, hippocampal neurons were transfected with GFP, Ncdn WT-GFP or Ncdn C3,4S-GFP at ~7 DIV. Twenty-four hours after transfection, neurons were treated with extracellular buffer (0.1% TritonX-100, 129 mM NaCl, 5 mM KCl, 2 mM CaCl₂, 1 mM MgCl₂, 20 mM Hepes at pH 7.4, 30 mM D-glucose) for 90 seconds prior to fixation with methanol (50). Neurons were immunostained with rabbit polyclonal anti-GFP and Alexa Fluor 488 goat anti-rabbit IgG (Invitrogen A11034).

Validation of DHHC1 and 10 knockdown vectors

HEK293 cells (5 x 10⁵ cells/6-wells dish) were co-transfected with 0.1 µg of pEF-BosHA:mDHHC1 or 10 plasmid and 2.0 µg of pCAGGS:EmGFP-miR-DHHC1_532, miR-DHHC1_911, miR-DHHC10_171, or miR-DHHC10_312 by Lipofectamine Plus reagent. Sixty hours after transfection, HEK293 cells were lysed in SDS-PAGE sample buffer (62.5mM Tris/Cl at pH 6.8, 10% glycerol, 2% SDS, and 0.001% bromophenol blue) with 2-ME and boiled at 100°C for 5 minutes. The samples were subjected to SDS-PAGE and Western blotting with the indicated antibodies.

Knockdown study of DHHC 1, 3 and 10 in hippocampal neurons

Hippocampal neurons were transfected with pCAGGS:EmGFP-miRNA-LacZ (miR-LacZ),

miR-DHHC1_532, miR-DHHC3_735, or miR-DHHC10_171 at 9-16 DIV by Lipofectamine 2000. About seven days after transfection, neurons were fixed with 4% paraformaldehyde/120 mM sucrose/100 mM Hepes at pH 7.4 for 10 minutes and immunostained with rabbit polyclonal anti-Ncdn and mouse monoclonal anti-MAP2 as described above. Knocked-down neurons were visualized by GFP. The dendrites (30-50 μm from the cell body) were traced by polyline drawing, and the average intensity of Ncdn in the dendrites was quantified by ZEN software of Zeiss LSM5. The average intensity of Ncdn was normalized to the average intensity of MAP2. The results are expressed as mean \pm SE. Statistical comparisons between groups were performed by the Student's t test.

Results

***In silico* proteomics screening for novel palmitoyl substrates**

Identification of palmitoyl substrates is important for elucidating physiological roles of protein palmitoylation. The recent development of the acyl-biotinyl exchange (ABE) method, which biochemically purifies palmitoylated proteins from tissue samples, enables the comprehensive profiling of palmitoylated proteins (4, 21). Combining the ABE method with mass spectrometry (ABE-MS method), more than 200 new palmitoyl protein candidates were recently identified (4). However, this approach is unsuitable for several proteins, 1) which are hardly extracted from the membrane fraction by 2% SDS for ABE purification, 2) which are expressed at too low level in tissues or cells to be identified by mass spectrometry analysis, and 3) which are highly post-translationally modified and hardly ionized for mass spectrometry analysis. By the ABE method, non-palmitoylated proteins (false positive), which tightly associate with palmitoyl proteins, may be co-purified. Furthermore, no information about palmitoylation sites is available.

To complementarily overcome those weak points of ABE-MS method, I took advantage of computational prediction using clustering and scoring strategy (CSS)-Palm 2.0 algorithm, which was recently developed by Yao's group for palmitoylation-site prediction (45) and freely available at <http://csspalm.biocuckoo.org/index.php>. To evaluate whether CSS-Palm 2.0 correctly predicts real palmitoylation sites, I performed a pilot study using known palmitoyl-proteins and non-palmitoyl proteins. CSS-Palm 2.0 showed high scores toward

representative palmitoyl substrates (*e.g.*, PSD-95, 5.096; GAP-43, 16.844; H-Ras, 4.024), but lower scores toward non-palmitoyl proteins (actin, 1.296; β -catenin, 0.687). This inspired me to apply the comprehensive protein sequences to CSS-Palm 2.0 (*in silico* proteomics), yielding a lot of novel palmitoyl substrates.

As a comprehensive protein database, I used the UniProt database (<http://www.uniprot.org/>) and selected *mus musculus* as an organism, which contains more than 60,000 protein sequences. The total number of the protein sequences is much larger than that of the mouse genes (about 30,000 genes) because splicing variants and redundancies with different accession numbers are included in the database. To automatically retrieve protein sequences from UniProt database and apply them to CSS-Palm 2.0 prediction program, my colleague, Naoki Takahashi, and I developed the automatic program (see Materials and Methods) and ran it over one week. Proteins that have cysteines with CSS-Palm score >0 were listed up (the result was uploaded at <http://www.nips.ac.jp/fukata/palm2>). I noted that most of known palmitoylated substrates showed more than score 1.8 and set 1.8 as the cut-off value. Because of our interest in neuronal proteins, brain enrichment score (See Materials and Methods) was used as another criterion for selection (cut-off point is >0.75) and about 750 proteins were listed up as candidates for neuronal palmitoyl substrates. I finally selected 17 interesting proteins as candidates for novel palmitoyl substrates, based on their brain enrichment and the idea that palmitoylated proteins accumulate at specialized membrane compartments, like postsynaptic membranes, presynaptic membranes,

focal adhesions and tight junctions (**Table 3**).

At the postsynapse, many proteins are subjected by protein palmitoylation, which regulates their localization and function (1, 3, 4). Examples include AMPA-type glutamate receptor (AMPA) (51, 52), NMDA-type receptor (53) and their scaffolding proteins, PSD-95 (28), PSD-93 (54) and GRIP (55). As AMPAR, which mediates fast excitatory synaptic transmission in brain (56), and its regulatory proteins are palmitoylated, I assumed that other AMPAR regulators with high CSS-Palm scores might be palmitoylated. I selected transmembrane AMPAR regulatory protein TARP γ 2 (CSS-Palm score; 1.913) (57-61), TARP γ 8 (2.461) (57-59), cornichon-2 (CNIH2) (2.266) (62), and CaMKII α (3.765) (63-65) as novel candidates for palmitoyl substrates (**Table 3**). In addition, kalirin7, a Rho guanine nucleotide exchange factor and PSD-95-binding protein (2.297) (66), and homer 1C (2.687) (67, 68), a regulator of group I mGluRs, were selected. Neurochondrin (Ncdn)/Norbin (13.016) (39), a regulator for metabotropic glutamate receptor 5 (mGluR5), was also selected.

At the presynapse, numerous SNARE proteins including SNAP-25, synaptotagmin, synaptobrevin, and syntaxin, have been reported as palmitoyl substrates (4). Besides SNARE proteins, I focused on three important presynaptic proteins with high CSS-Palm scores; Rab3A (CSS-Palm score; 2.313), Syd-1 (3.078) and liprin- α 2 (Syd-2) (4.783) (**Table 3**). Rab3A is a representative Rab small GTPase and a primary regulator of synaptic vesicle fusion process (69).

Syd-1 (for synaptic defect) and Syd-2 were originally identified as mutants in *Caenorhabditis elegans* (70, 71). Syd-2 mutant shows significantly lengthened active zones and the mammalian Syd-2 homologue liprins also localize at the presynaptic membranes and function as the master assembly molecules that recruit numerous synaptic components to presynaptic sites (70). Syd-1, a putative Rho-GTPase activating protein, localizes at the presynaptic terminal and may be involved in specifying axon identity during initial polarity acquisition (71).

At cell adhesion sites, integrins at focal adhesions (72) and claudins at tight junctions (73) are palmitoylated. I speculate that scaffolding/anchoring proteins at these adhesion sites may also be palmitoylated and contribute to generation and maintenance of the membrane specialization. I selected paxillin (CSS-Palm score; 2.278) and zyxin (1.952) as the candidates at focal adhesion and Par3 (3.061) as the candidate at tight junction.

Also, I have interests in several functional molecules with high CSS-Palm scores, including TRPM8 (CSS-Palm score; 1.913) and TRPC1 (2.547) (members of transient receptor potential (TRP) channels), orexin receptor type2 (G-protein coupled receptor) (3.500) and KIF5C (Kinesin motor protein) (2.183). Although many of ion channels are palmitoylated, palmitoylation of the TRP channel superfamily has not been reported. The fact that TRP channels in heterologous cells are not efficiently trafficked to cell surface (74) suggests the involvement of palmitoylation in TRP trafficking process.

Confirmation of novel palmitoyl substrates by experimental approaches

Next, I examined whether those 17 substrate candidates were actually palmitoylated in cultured cells. First, I isolated candidate cDNAs by RT-PCR or collected some of them from other researchers (**Table 2**). Then, I transfected the individual candidate cDNAs together with DHHC3 palmitoylating enzyme into HEK293 cells and assessed palmitoylation of candidate proteins by metabolic labeling with [³H]palmitate. Based on our previous studies, DHHC3 functions as a general palmitoylating enzyme (*i.e.*, all palmitoyl-substrates we have tested are palmitoylated by DHHC3) (3). Among postsynaptic candidate proteins, TARP γ 2, TARP γ 8, CNIH2, CaMKII α , and Ncdn were robustly palmitoylated (**Figure 2A**). Neither kalirin7 nor homer 1C were palmitoylated (**Figure 2A**). A presynaptic candidate, Syd-1, but neither Rab3A nor liprin- α 2, was palmitoylated. Liprin- α 2 expression was not confirmed, because an antibody to liprin- α 2 was not available and tagging was not possible at present as potential palmitoyl cysteines are located at both termini of liprin- α 2. Liprin- α 2 palmitoylation will need further assessment. Among cell adhesion-related proteins, zyxin incorporated [³H]palmitate, but neither paxillin nor Par3 did. TRPM8, TRPC1 and orexin receptor type2 were efficiently palmitoylated by DHHC3. Thus, I identified 10 palmitoyl-substrates from the 17 candidates. However, this assay might include false positive substrates, as both DHHC3 enzyme and a substrate protein are overexpressed in cells. Next, I tested whether *endogenous* proteins are palmitoylated in neurons by ABE method, which requires specific antibodies to substrates. I examined whether

endogenous TARP γ 8, CaMKII α , Ncdn and Syd-1 are palmitoylated because their antibodies were available (Ncdn antibody established in this study was described below in detail) and found that those four proteins were palmitoylated in the primary hippocampal neurons (**Figure 2B**). Although I could not examine the rest of the candidates (TARP γ 2, CNIH2, zyxin, TRPM8, TRMC1, and orexin receptor type2), this result strongly suggests that these candidates may be authentic palmitoyl-substrates.

DHHC1, 3, 7 and 10 enhance Ncdn palmitoylation

Next my interest was which DHHC proteins palmitoylate these substrates. To identify the responsible enzymes for Ncdn, TARP γ 8, CaMKII α and Syd-1, I screened DHHC palmitoylating enzyme library by metabolic labeling with [3 H]palmitate (10, 23). Palmitoylation of all four substrates was enhanced by DHHC3 and DHHC 7, which belong to the same subfamily (**Figure 1B and 3**). In addition to DHHC3 and DHHC7, Ncdn was also palmitoylated by DHHC1 and DHHC10 (**Figure 3**), which belong to another subfamily (**Figure 1B**). Syd-1 was palmitoylated very weakly by DHHC14 (**Figure 3A**). TARP γ 8 was also palmitoylated very weakly by DHHC2 and 15, which belong to the same subfamily (**Figure 1B and 3A**). Importantly, Ncdn is the first substrate for DHHC1/10 subfamily (75). Because Ncdn is predominantly expressed in brain and has very high CSS-Palm score (**Figure 4B**) and plays an important role in neurite-outgrowth (35, 43) and synaptic plasticity (35, 38, 39), I focused on this substrate-enzyme pair in the subsequent study.

Palmitoylation of Ncdn occurs at cysteines 3 and 4

Ncdn protein contains 25 cysteine residues, two near the amino (N)-terminus at positions 3 and 4 and other cysteines scattered throughout the protein. CSS-Palm 2.0 suggests cysteines 3 and 4 are highly potential for Ncdn palmitoylation sites (**Figure 4A**). The scores are 13.016 and 12.562 at Cys-3 and Cys-4, respectively. In contrast, the scores of the other cysteines are less than 1.8 cut-off value. These scores of Cys-3 and Cys-4 of Ncdn are much higher than those of the other novel substrates, TARP γ 8 (2.461), CaMKII α (3.765), and Syd-1 (3.078) and even a well-known substrate, PSD-95 (5.096) (**Table 3** and **Figure 4B**). In fact, the CSS-Palm score of Ncdn (13.016) is the 7th highest candidate out of proteins with high brain enrichment score (>0.75) (**Table 4** and **Figure 4B**). To determine whether Cys-3 or Cys-4 or both in Ncdn serves as the palmitoylation site, I generated mutants of Ncdn in which either one or both of those cysteine residues were mutated to serine (Ncdn C3S, Ncdn C4S and Ncdn C3,4S). HEK293 cells transfected with these mutant constructs or wild-type Ncdn together with DHHCs were metabolically labeled with [3 H]palmitate. Fluorography showed that mutation of either Cys-3 or Cys-4 or dual mutations completely eliminated palmitoylation of Ncdn (**Figure 4C**). It is not clear why either mutation of the two cysteines completely blocks palmitoylation of the protein, but palmitoylation of certain other proteins also requires two closely adjacent cysteines (76). Also, I found that the palmitoylation sites, Cys-3 and Cys-4, were shared with DHHC1, 2, 3, 7, and 10. These results indicate that Ncdn palmitoylation sites are Cys-3 and Cys-4, and that

DHHC1, 2, 3, 7, and 10 mediate the Ncdn palmitoylation.

Because it was reported that some palmitoyl substrates physically interact with their responsible enzymes (77-79), I tested the interaction of Ncdn with DHHC2, 3, and 10. Hisx6-Flag-tagged DHHC2, 3 and 10 were expressed in HEK293 cells and the lysates were mixed with rat brain extracts containing endogenous Ncdn. Hisx6-Flag-DHHC proteins were tandem affinity-purified with anti-Flag-antibody-conjugated M2 agarose and subsequently with Ni-NTA agarose. The purified samples were analyzed by Western blotting with anti-Ncdn antibody. DHHC10, but not DHHC3, preferentially interacted with Ncdn (**Figure 4D**). Although DHHC1 was not extracted from the membrane fractions (not shown), this result suggests that DHHC1/10 subfamily stably interacts with Ncdn, whereas DHHC3/7 subfamily palmitoylates Ncdn by the transient interaction. We also found that DHHC1/10 subfamily specifically palmitoylates Ncdn, under the conditions in which DHHC3/7 subfamily palmitoylates $G\alpha_q$ and GluA2 as well as Ncdn (**Figure 4E**). Thus, DHHC3/7 subfamily and 1/10 subfamily may differently regulate palmitoylation states of Ncdn.

I next investigated how DHHC1/10 subfamily recognizes Ncdn as their specific substrate. Because previously reported palmitoylation sites often occur in the N-terminal region (*e.g.*, PSD-95 at Cys-3 and Cys-5; GAP43 at Cys-3 and Cys-4), and GFP-tagging to the N-terminus of the protein completely blocks its palmitoylation (76), I first examined whether DHHC1/10

subfamily recognizes the N-terminal cysteines of Ncdn. GFP was added to either the N- or C-terminus of Ncdn and each GFP tagged Ncdn was tested for palmitoylation by metabolic labeling assay (**Figure 4F**). The C-terminal GFP-tagged Ncdn, containing the intact N-terminal palmitoylation sites (Cys-3 and Cys-4), was palmitoylated by both DHHC3 and 10. In contrast, palmitoylation of the N-terminal GFP-tagged Ncdn, where palmitoyl cysteines are located in the internal region of the expressed protein, was completely abolished, indicating that the palmitoyl cysteines have to be located at the N-terminal region of Ncdn for both DHHC3 and 10. I next examined the minimum sequence required for recognition by DHHC10. The N-terminal short peptides of Ncdn with the C-terminal GFP-tag were tested for palmitoylation by metabolic labeling assay (**Figure 4G**). The N-terminal four-amino acid peptide, MSCC (Met-Ser-Cys-Cys, N4) and longer (N5) were palmitoylated while the N-terminal three-amino acid peptide, MSC (Met-Ser-Cys, N3) was no longer palmitoylated by DHHC3 and 10. This is consistent with the result that the single Cys is not enough for palmitoylation (**Figure 4C**). Although the present study could not see robust differences in substrate recognitions of DHHC3 and 10 subfamilies, it will be a next important study whether there is a specific rule of substrate recognition for DHHC1/10 subfamily (also see Discussion).

DHHC1/10 subfamily is localized in dendritic shafts and dendritic spines

DHHC2/15 subfamily and DHHC3/7 subfamily showed different localization in neurons (47). To investigate the localization of the novel functional subfamily, DHHC1/10, in neurons,

HA-tagged DHHC1 and 10 were transfected into cultured hippocampal neurons, and neurons were doubly stained with anti-HA and anti-PSD-95 antibodies. HA-tagged DHHC1 and 10 were observed in the cell body and dendrites and partially co-localized with postsynaptic PSD-95 in the dendritic spines (**Figure 5A**). Under the conditions, the other subfamily of Ncdn palmitoylating enzymes, DHHC3/7, was specifically localized in the Golgi apparatus as previously described (**Figure 5B**) (23, 47). I also compared with other DHHC subfamilies and found that DHHC2/15 subfamily distributed in dendrites and mainly localized as small vesicular-like structures (**Figure 5C**) (47, 80). DHHC5/8 subfamily, especially DHHC5, was localized at the plasma membrane in dendrites (**Figure 5D**). Thus, DHHC proteins show the subfamily-specific distributions in neurons and DHHC1/10 subfamily is localized in dendrites and dendritic spines.

Ncdn is localized specifically in dendrites in neurons

To examine the subcellular localization of Ncdn in neurons, I generated an antibody against the N-terminal 59 amino acids of Ncdn (N-rNcdn). A single band with ~75 kDa of molecular weight was detected in mouse and rat brain lysates and rat cultured hippocampal and cortical neuron lysates by Western blotting with anti-Ncdn (**Figure 6A**). In cultured cortical neurons, Ncdn expression was hardly detected at 3 DIV, when an axon just differentiates from the immature neurite (**Figure 6B**). Ncdn expression began to be detected at 7 DIV and was the highest at 14 DIV, when dendrites differentiate from the other immature neurites and become thicker, longer

and branched. Ncdn expression declined but was higher at 21-28 DIV, when synapses develop, than at 7 DIV. Ncdn was still expressed in 1-2 month old culture. Importantly, this expression pattern of Ncdn in cultured neurons was very similar to that of mGluR5. Subcellular distribution of Ncdn was examined by biochemically fractionating the brain homogenate (**Figure 6C**). Ncdn protein was fractionated into both cytoplasmic (S3) and membrane fractions (P2), and was further fractionated into both TritonX-100-soluble (Sol1) and -insoluble (PSD1 and PSD2) fractions from P2-derived synaptosome fraction. Fractionation was successful, as a postsynaptic marker protein, PSD-95, was fractionated exclusively into PSD fractions. Ncdn was similarly enriched in S3 and PSD fractions, suggesting that there are two major pools, palmitoylated and non-palmitoylated Ncdn.

Next, to examine Ncdn localization in neurons by immunofluorescent study with anti-Ncdn antibody, the knockdown vector for rat Ncdn was constructed (miR-Ncdn). miR-Ncdn803 effectively reduced expression of Ncdn-HA in transfected HEK cells (**Figure 7A**), and was used in cortical neurons (**Figure 7B**). Strong somato-dendritic signals of the Ncdn antibody were observed in control neurons (**Figure 7B**). This staining signal was specific as knockdown of Ncdn completely abrogated the staining with this antibody (**Figure 7B**). Using this antibody, I next examined whether Ncdn is localized in dendrites and/or an axon. Anti-MAP2 and pan-axonal neurofilament (NF) antibodies were used as a dendrite marker and an axonal marker, respectively. Ncdn was localized in MAP2-positive dendrites, whereas Ncdn was completely

absent in the NF-positive axon (**Figure 7C**). In dendrites, Ncdn was partially co-localized with PSD-95 and apposed to presynaptic synaptophysin (**Figure 7D**). Given that Ncdn physically interacted with DHHC10 (**Figure 4D**) and that DHHC1/10 subfamily was localized in dendritic shafts and dendritic spines (**Figure 5A**), this novel palmitoyl substrate-enzyme pair may be co-localized in dendritic spines. In fact, endogenous Ncdn and HA-DHHC10 were co-localized in dendritic spines (**Figure 7E**). Consistent with this, Ncdn WT-GFP was relocated to a perinuclear domain when DHHC10 was co-expressed in COS7 cells, whereas Ncdn was distributed diffusely in COS7 cells with DHHC3 (**Figure 7F**). DHHC10-induced redistribution of Ncdn required the critical cysteines of Ncdn (**Figure 7F**; Ncdn C3,4S). These results indicate that DHHC1/10 subfamily may redistribute Ncdn by palmitoylating activity and physical interaction.

Localization of Ncdn in the membrane structure of dendrites is regulated by its palmitoylation

To investigate a role of palmitoylation in Ncdn localization, the C-terminal GFP-tagged wild type (WT) Ncdn and palmitoylation-deficient mutant (Ncdn C3,4S) were expressed in hippocampal neurons. Both Ncdn WT and Ncdn C3,4S distributed diffusely in dendrites and the cell body, and the difference in their localizations was not clearly observed (**Figure 8A**). The extremely high expression of both Ncdn WT-GFP and Ncdn C3,4S-GFP may mask the difference. To remove the soluble/cytosolic Ncdn from the cells, neurons were pretreated with

0.1% Triton-X before fixation (50). Only Ncdn WT-GFP signals remained in the cell body and dendrites and were observed at somatic plasma membrane and in dendrites as small puncta (**Figure 8B**). Under the conditions, GFP and palmitoylation-deficient mutant were easily extracted from the dendrites. This strongly suggests that palmitoylation is necessary for Ncdn localization to dendritic membrane structures.

Knockdown of DHHC1 expression suppresses dendritic localization of Ncdn

I found that Ncdn is palmitoylated by both DHHC1/10 and DHHC3/7 subfamilies. To examine whether these DHHC proteins regulate functions and localization of Ncdn. I knocked-down DHHC1, 3, and 10 in hippocampal neurons. DHHC7 was excluded because DHHC7 is expressed at a negligible level in hippocampal neurons (47). Knockdown of DHHC1 and 10 was verified in HEK293 cells by co-transfection of DHHCs and miR-DHHC constructs (**Figure 9A**). DHHC3 knockdown was previously reported (23, 47). Hippocampal neurons were transfected with miRNA constructs, miR-LacZ, miR-DHHC1_532, miR-DHHC3_735 or miR-DHHC10_171 at 9-16 DIV, when neurons develop dendrites. Neurons were stained with anti-Ncdn antibody together with anti-MAP2 antibody around 20 DIV, when neurons establish dendritic arbors and synapses. When DHHC1 was knocked-down, the intensity of Ncdn in dendrites significantly decreased (**Figure 9B and C**). In contrast, knockdown of DHHC3 and DHHC10 had no effects on dendritic localization of Ncdn (**Figure 9B and C**). This result suggests that Ncdn palmitoylation by DHHC1 regulates dendritic localization of Ncdn. This is

consistent with the observation that palmitoylation-deficient mutant was easily extracted from membrane structures in dendrites by pretreatment of 0.1% Triton-X 100 before fixation (**Figure 8B**). Thus, Ncdn palmitoylation by DHHC1 plays an important role in dendritic localization of Ncdn.

Discussion

***In silico* prediction of palmitoyl proteins**

The recent development of purification methods for palmitoylated proteins (ABE method or click chemistry) greatly contributed to identification of novel palmitoyl-proteins (4, 20, 21, 29, 30). However, these methods possess several potential problems that could lead to false-negative or false-positive results. The biochemical properties of proteins, such as detergent insolubility and posttranslational modifications, could sometimes hinder the purification and the mass spectrometry analysis, leading to false negative results. Also, non-palmitoylated proteins might be co-purified with palmitoyl-substrates, leading to false positive results. In fact, non-palmitoylated, secreted protein LGI1, which indirectly associates with palmitoylated PSD-95 through ADAM22, was listed as a candidate for palmitoyl-proteins (4). In this study, I screened for novel palmitoyl substrates through *in silico* proteomics by CSS-Palm 2.0 prediction program, which requires only protein sequences and does not consider any biochemical properties of target proteins. By automatically applying all mouse protein sequences to CSS-Palm 2.0, I lined up the obtained 59,136 protein sequences according to the CSS-Palm scores. In fact, this list included many transmembrane proteins, such as G-protein coupled receptors, some of which are difficult to be analyzed by mass spectrometry. I selected the 17 interesting candidates and experimentally identified the novel 10 palmitoyl substrates that were not captured by the ABE or click chemistry method. This indicates that *in silico* approach is useful for the discovery of novel palmitoyl substrates and complementally functions with

previous experimental methods. However, of the 17 candidates, the 7 proteins were failed in the confirmation test by metabolic labeling assay (false-positive results). In terms of the accuracy of the prediction, this prediction program has room for improvement. CSS-Palm 2.0 was developed by referring 263 palmitoylation sites from 109 proteins, which had been experimentally shown (45). As the number of references of known substrates and their palmitoylation sites increases, more accurate prediction can be expected.

Consensus sequences of protein palmitoylation

The consensus sequence of palmitoylation sites remains to be elucidated while those of other lipid modifications, myristoylation and isoprenylation, are defined (81, 82). Myristoylation reaction is directed at the Gly residue located at the N-terminal end of the proteins ($\underline{M}GXXXXS/T$, where G is myristoylation site and X is any amino acid) (81). The Cys residue in the C-terminal motif in the $\underline{C}AAX$, where A is aliphatic amino acid and X is any amino acid, is known as the consensus isoprenylation site (82). In contrast, palmitoylation occurs at the various Cys residues located at 1) the N-terminal region in PSD-95, GAP-43, and Ncdn (in this study), 2) the internal region in SNAP-25 and CSP, 3) the C-terminal region in H-Ras and Cdc42, and 4) the juxtamembrane region of various transmembrane proteins in NCAM and GluAs (3). I hypothesize that the large family of DHHC proteins with at least 10 subfamilies may explain for diverse palmitoylation motifs. The individual DHHC subfamily may recognize a specific pattern for palmitoylation as individual protein kinases recognize specific substrate sequences for their

phosphorylation. In fact, our group found that 1) DHHC2/15 subfamily specifically palmitoylates PSD-95 and GAP-43, both of which have hydrophobic residues and basic residues surrounding the palmitoyl N-terminal Cys residues (**Figure 1B**) (10, 76), 2) DHHC3/7 subfamily shows broader substrate specificity than other members and often palmitoylates juxtamembrane Cys residues of transmembrane proteins (**Figure 1B**) (10, 79, 83), 3) DHHC9/DHHC18 subfamily favors dual-lipidated substrates with palmitoylated Cys residues near the C-terminal isoprenylated cysteine (H-Ras and N-Ras) (**Figure 1B**) (10, 26), 4) DHHC21 palmitoylates Cys residues located near the N-terminal myristoyl Gly residue (LCK, $G\alpha_{i2}$ and eNOS) (**Figure 1B**) (23, 78), and 5) DHHC17 favorably acts on proteins containing the internal Cys-rich motif and also sometimes Cys with an adjacent proline residue (SNAP-25, CSP and huntingtin) (84-86). Here, I discovered that DHHC1/10 subfamily members also function as palmitoylating enzymes and identified Ncdn as the first substrate for DHHC1/10. Because DHHC1/10 subfamily has not shown any enzymatic activities to proteins with the specific palmitoyl motif described above, I assumed that DHHC1/10 might also have a distinct rule for substrate recognition. Analysis of Ncdn deletion mutants showed the N-terminal four amino acids (MSCC-) are sufficient for palmitoylation (**Figure 4G**). This very short consensus needs to occur at the extreme N-terminus (**Figure 4F**). Further studies by mutagenesis in the second Ser residue (MSCC-) will contribute to clarifying the precise DHHC1/10-specific consensus sequence. If CSS-Palm 2.0 (currently updated to CSS-Palm 3.0) takes “DHHC subfamily-specific rules” into account for its programming, the software should become a much powerful tool for palmitoylation prediction.

Physiological roles of Ncdn palmitoylation

Dendritic localization of Ncdn

In this study, I found that Ncdn, a neuron-specific protein, is a novel palmitoyl substrate and localized at the cell body, dendritic shafts and dendritic spines, but not in the axon. This suggests that Ncdn is synthesized at the cell body, specifically traffics into dendrites and is finally targeted to the dendritic spines. I found that knocked-down of DHHC1 reduces Ncdn in dendrites (**Figure 9B and C**) and that palmitoylation-deficient mutant of Ncdn (Ncdn C3,4S) cannot arrive at membrane structures in dendrites (**Figure 8B**). These results indicate that palmitoylation by DHHC1 is necessary for dendritic localization of Ncdn. Although in heterologous HEK293 cells DHHC10 is more potent for Ncdn palmitoylation than DHHC1, the knockdown study of DHHC1 showed that DHHC1 is a physiological PAT for Ncdn at least in hippocampal neurons (**Figure 9B and C**). The next question is where in neurons DHHC1 palmitoylates Ncdn. If DHHC1 is enriched in the dendritic spines, DHHC1 may actively recruit Ncdn to the spines. Although exogenous expressed DHHC1 presents somato-dendritic distribution including dendritic spines (**Figure 5A**), the precise localization of endogenous DHHC1 remains unclear. In general, DHHC proteins are expressed at very low levels in cells and have four or six transmembrane domains (**Figure 1A**). This implies the difficulty to generate the specific antibodies to DHHC proteins. To overcome this situation and obtain specific antibodies to DHHC1 and 10, I took advantage of baculovirus display method (87, 88), which is useful for

production of antibodies for complex membrane proteins and was successful for DHHC2 (47). Baculovirus particles expressing(/inserted with) Hisx6-Flag-full length DHHC1 or 10 on their envelopes together with small amounts of purified Hisx6-Flag-DHHC1 or 10 proteins were used as the antigens of mouse immunization. Very recently, I obtained monoclonal antibody clones against DHHC1, which detected recombinant DHHC1 by Western blotting and immunostaining (not shown). Further characterization of these antibodies combined with DHHC1-knockdown will clarify the specific localization of DHHC1 in neurons, and this should reveal where DHHC1 palmitoylates Ncdn and regulates its distribution.

Neurite outgrowth and dendritogenesis

The previous studies showed that overexpression of Ncdn promotes neurite-outgrowth in Neuro2a cells (35, 43). The first 100 amino acids of Ncdn, including palmitoylation sites, contain the activity necessary to induce this phenomenon (43). In polarized neurons, Ncdn protein is highly expressed during dendrite arborization (**Figure 6B**), and localized specifically in dendrites (**Figure 6C**). These imply that Ncdn is involved in dendritogenesis. Interestingly, I preliminary found that knockdown of DHHC1 or Ncdn at earlier DIV (~7 DIV) tends to shorten the dendritic length (not shown), suggesting that the amount of Ncdn in dendrites regulates dendrite elongation. As Ncdn interacts with Dia1 (43), an actin nucleation factor (44), Ncdn palmitoylation may regulate dendritogenesis through recruiting Dia1 near the plasma membranes.

Synaptic plasticity

Ncdn was originally identified as an inducible gene during LTP induction (35). Very recently, Greengard's group showed that Ncdn interacts with mGluR5 and increases the cell surface expression of mGluR5 (39). Forebrain-specific Ncdn KO mice show the reduction of DHPG-induced LTD and the impairment of the induction of LTP in the Schaffer collateral to CA1 synapses (39). I assumed that palmitoylation of Ncdn is involved in this process and examined whether DHHC10-induced palmitoylation of Ncdn enhances the surface expression of mGluR5 in HEK293 heterologous cells. However, I could not reproduce the effect of Ncdn on the mGluR5 surface expression under the conditions in which TARP γ 2 dramatically enhances surface expression of GluA1 (not shown). Because Greengard's group used Neuro2a cells, this discrepancy might be due to the difference in cell types.

Perspectives

Besides Ncdn, I identified interesting palmitoyl substrates including Syd-1, TARPs, CNIH2, CaMKII α , TRP channels and zyxin. Especially, I have interests with Syd-1 and TRP channels because Syd-1 was reported as a determinant of presynaptic specialization in *Caenorhabditis elegans* and palmitoylation of Syd-1 may play a central role in Syd-1 recruitment to presynaptic sites. Because TRP channel activity is regulated by cysteine *S*-nitrosylation via nitric oxide (89), it seems worthy to examine whether palmitoylation sites overlaps with these *S*-nitrosylation sites

and palmitoylation affects channel activity of TRP.

In conclusion, I challenged systematic identification of palmitoyl substrates by *in silico* computational approach and identified unexpected substrates. Among them, I focused on the Ncdn palmitoylation and found that DHHC1/10 subfamily and DHHC3/7 subfamily enhance the Ncdn palmitoylation in cells. DHHC1 physiologically regulates Ncdn distribution to dendrites in hippocampal neurons. I believe that such *in silico* approach should function cooperatively with conventional experimental approaches.

References

1. El-Husseini, A. el-D. and Brecht, D. S. (2002) *Nat Rev Neurosci* **3**, 791-802
2. Resh, M. D. (2006) *Nat Chem Biol* **2**, 584-590
3. Fukata, Y. and Fukata, M. (2010) *Nat Rev Neurosci* **11**, 161-175
4. Kang, R., Wan, J., Arstikaitis, P., Takahashi, H., Huang, K., Bailey, A. O., Thompson, J. X., Roth, A. F., Drisdell, R. C., Mastro, R., Green, W. N., Yates, J. R., Davis, N. G., and El-Husseini, A. (2008) *Nature* **456**, 904-909
5. Lobo, S., Greentree, W. K., Linder, M. E., and Deschenes, R. J. (2002) *J Biol Chem* **277**, 41268-41273
6. Zhao, L., Lobo, S., Dong, X., Ault, A. D., and Deschenes, R. J. (2002) *J Biol Chem* **277**, 49352-49359
7. Roth, A. F., Feng, Y., Chen, L., and Davis, N. G. (2002) *J Cell Biol* **159**, 23-28
8. Bartels, D. J., Mitchell, D. a, Dong, X., and Deschenes, R. J. (1999) *Mol Cell Biol* **19**, 6775-6787
9. Hemsley, P. a and Grierson, C. S. (2008) *Trends Plant Sci* **13**, 295-302
10. Fukata, M., Fukata, Y., Adesnik, H., Nicoll, R. a, and Brecht, D. S. (2004) *Neuron* **44**, 987-996
11. Oyama, T., Miyoshi, Y., Koyama, K., Nakagawa, H., Yamori, T., Ito, T., Matsuda, H., Arakawa, H., and Nakamura, Y. (2000) *Genes Chromosomes Cancer* **29**, 9-15

12. Mukai, J., Liu, H., Burt, R. a, Swor, D. E., Lai, W.-S., Karayiorgou, M., and Gogos, J. a
(2004) *Nat Genet* **36**, 725-731
13. Chen, W.-Y., Shi, Y.-Y., Zheng, Y.-L., Zhao, X.-Z., Zhang, G.-J., Chen, S.-Q., Yang, P.-D.,
and He, L. (2004) *Hum Mol Genet* **13**, 2991-2995
14. Mukai, J., Dhillia, A., Drew, L. J., Stark, K. L., Cao, L., MacDermott, A. B., Karayiorgou, M.,
and Gogos, J. a (2008) *Nat Neurosci* **11**, 1302-1310
15. Mansouri, M. R., Marklund, L., Gustavsson, P., Davey, E., Carlsson, B., Larsson, C., White,
I., Gustavson, K.-H., and Dahl, N. (2005) *Eur J Hum Genet* **13**, 970-977
16. Raymond, F. L., Tarpey, P. S., Edkins, S., Tofts, C., O'Meara, S., Teague, J., Butler, A.,
Stevens, C., Barthorpe, S., Buck, G., Cole, J., Dicks, E., Gray, K., Halliday, K., Hills, K.,
Hinton, J., Jones, D., Menzies, A., Perry, J., Raine, K., Shepherd, R., Small, A., Varian, J.,
Widaa, S., Mallya, U., Moon, J., Luo, Y., Shaw, M., Boyle, J., Kerr, B., Turner, G.,
Quarrell, O., Cole, T., Easton, D. F., Wooster, R., Bobrow, M., Schwartz, C. E., Gecz, J.,
Stratton, M. R., and Futreal, P. A. (2007) *Am J Hum Genet* **80**, 982-987
17. Singaraja, R. R., Hadano, S., Metzler, M., Givan, S., Wellington, C. L., Warby, S., Yanai, A.,
Gutekunst, C.-A., Leavitt, B. R., Yi, H., Fichter, K., Gan, L., McCutcheon, K., Chopra, V.,
Michel, J., Hersch, S. M., Ikeda, J.-E., and Hayden, M. R. (2002) *Hum Mol Genet* **11**,
2815-2828

18. Huang, K., Yanai, A., Kang, R., Arstikaitis, P., Singaraja, R. R., Metzler, M., Mullard, A., Haigh, B., Gauthier-Campbell, C., Gutekunst, C.-A., Hayden, M. R., and El-Husseini, A. (2004) *Neuron* **44**, 977-986
19. Keller, C. a, Yuan, X., Panzanelli, P., Martin, M. L., Alldred, M., Sassoè-Pognetto, M., and Lüscher, B. (2004) *J Neurosci* **24**, 5881-5891
20. Yang, W., Di Vizio, D., Kirchner, M., Steen, H., and Freeman, M. R. (2010) *Mol Cell Proteomics* **9**, 54-70
21. Roth, A. F., Wan, J., Bailey, A. O., Sun, B., Kuchar, J. a, Green, W. N., Phinney, B. S., Yates, J. R., and Davis, N. G. (2006) *Cell* **125**, 1003-1013
22. Drisdell, R. C. and Green, W. N. (2004) *Biotechniques* **36**, 276-285
23. Tsutsumi, R., Fukata, Y., Noritake, J., Iwanaga, T., Perez, F., and Fukata, M. (2009) *Mol Cell Biol* **29**, 435-447
24. Fukata, Y., Iwanaga, T., and Fukata, M. (2006) *Methods* **40**, 177-182
25. Ponimaskin, E., Dityateva, G., Ruonala, M. O., Fukata, M., Fukata, Y., Kobe, F., Wouters, F. S., Delling, M., Brecht, D. S., Schachner, M., and Dityatev, A. (2008) *J Neurosci* **28**, 8897-8907
26. Swarthout, J. T., Lobo, S., Farh, L., Croke, M. R., Greentree, W. K., Deschenes, R. J., and Linder, M. E. (2005) *J Biol Chem* **280**, 31141-31148
27. Skene, J. H. and Virág, I. (1989) *J Cell Biol* **108**, 613-624
28. Topinka, J. R. and Brecht, D. S. (1998) *Neuron* **20**, 125-134

29. Martin, B. R. and Cravatt, B. F. (2009) *Nat Methods* **6**, 135-138
30. Yount, J. S., Moltedo, B., Yang, Y.-Y., Charron, G., Moran, T. M., López, C. B., and Hang, H. C. (2010) *Nat Chem Biol* **6**, 610-614
31. Mirza, S. P., Halligan, B. D., Greene, A. S., and Olivier, M. (2007) *Physiol Genomics* **30**, 89-94
32. Santoni, V., Molloy, M., and Rabilloud, T. (2000) *Electrophoresis* **21**, 1054-1070
33. Fu, Y., Xiu, L.-Y., Jia, W., Ye, D., Sun, R.-X., Qian, X.-H., and He, S.-M. (2011) *Mol Cell Proteomics*
34. Zhao, Z., Hou, J., Xie, Z., Deng, J., Wang, X., Chen, D., Yang, F., and Gong, W. (2010) *Protein J* **29**, 531-537
35. Shinozaki, K., Maruyama, K., Kume, H., Kuzume, H., and Obata, K. (1997) *Biochem Biophys Res Commun* **240**, 766-771
36. Wang, H., Nong, Y., Bazan, F., Greengard, P., and Flajolet, M. (2010) *Commun Integr Biol* **3**, 487-490
37. Mochizuki, R., Dateki, M., Yanai, K., Ishizuka, Y., Amizuka, N., Kawashima, H., Koga, Y., Ozawa, H., and Fukamizu, A. (2003) *Biochem Biophys Res Commun* **310**, 1219-1226
38. Dateki, M., Horii, T., Kasuya, Y., Mochizuki, R., Nagao, Y., Ishida, J., Sugiyama, F., Tanimoto, K., Yagami, K.-I., Imai, H., and Fukamizu, A. (2005) *J Biol Chem* **280**, 20503-20508

39. Wang, H., Westin, L., Nong, Y., Birnbaum, S., Bendor, J., Brismar, H., Nestler, E., Aperia, A., Flajolet, M., and Greengard, P. (2009) *Science* **326**, 1554-1557
40. Ohoka, Y., Hirotani, M., Sugimoto, H., Fujioka, S., Furuyama, T., and Inagaki, S. (2001) *Biochem Biophys Res Commun* **280**, 237-243
41. Francke, F., Ward, R. J., Jenkins, L., Kellett, E., Richter, D., Milligan, G., and Bächner, D. (2006) *J Biol Chem* **281**, 32496-32507
42. Ward, R. J., Jenkins, L., and Milligan, G. (2009) *J Neurochem* **109**, 182-192
43. Schwaibold, E. M. C. and Brandt, D. T. (2008) *Biochem Biophys Res Commun* **373**, 366-372
44. Li, F. and Higgs, H. N. (2003) *Curr Biol* **13**, 1335-1340
45. Ren, J., Wen, L., Gao, X., Jin, C., Xue, Y., and Yao, X. (2008) *Protein Eng Des Sel* **21**, 639-644
46. Fukata, Y., Tzingounis, A. V., Trinidad, J. C., Fukata, M., Burlingame, A. L., Nicoll, R. a, and Brecht, D. S. (2005) *J Cell Biol* **169**, 399-404
47. Noritake, J., Fukata, Y., Iwanaga, T., Hosomi, N., Tsutsumi, R., Matsuda, N., Tani, H., Iwanari, H., Mochizuki, Y., Kodama, T., Matsuura, Y., Brecht, D. S., Hamakubo, T., and Fukata, M. (2009) *J Cell Biol* **186**, 147-160
48. Alexander, J. K., Govind, a P., Drisdell, R. C., Blanton, M. P., Vallejo, Y., Lam, T. T., and Green, W. N. (2010) *J Mol Neurosci* **40**, 12-20
49. Carlin, R. K., Grab, D. J., Cohen, R. S., and Siekevitz, P. (1980) *J Cell Biol* **86**, 831-845
50. Dresbach, T. (2003) *Mol Cell Neurosci* **23**, 279-291

51. Nicoll, R. a, Tomita, S., and Brecht, D. S. (2006) *Science* **311**, 1253-1256
52. Hayashi, T., Rumbaugh, G., and Huganir, R. L. (2005) *Neuron* **47**, 709-723
53. Hayashi, T., Thomas, G. M., and Huganir, R. L. (2009) *Neuron* **64**, 213-226
54. El-Husseini, a E., Topinka, J. R., Lehrer-Graiwer, J. E., Firestein, B. L., Craven, S. E., Aoki, C., and Brecht, D. S. (2000) *J Biol Chem* **275**, 23904-23910
55. DeSouza, S., Fu, J., States, B. a, and Ziff, E. B. (2002) *J Neurosci* **22**, 3493-3503
56. Shepherd, J. D. and Huganir, R. L. (2007) *Annu Rev Cell Dev Biol* **23**, 613-643
57. Tomita, S., Fukata, M., Nicoll, R. a, and Brecht, D. S. (2004) *Science* **303**, 1508-1511
58. Jackson, A. C. and Nicoll, R. a (2011) *Neuron* **70**, 178-199
59. Chen, L., Chetkovich, D. M., Petralia, R. S., Sweeney, N. T., Kawasaki, Y., Wenthold, R. J., Brecht, D. S., and Nicoll, R. a (2000) *Nature* **408**, 936-943
60. Hashimoto, K., Fukaya, M., Qiao, X., Sakimura, K., Watanabe, M., and Kano, M. (1999) *J Neurosci* **19**, 6027-6036
61. Tomita, S., Chen, L., Kawasaki, Y., Petralia, R. S., Wenthold, R. J., Nicoll, R. a, and Brecht, D. S. (2003) *J Cell Biol* **161**, 805-816
62. Schwenk, J., Harmel, N., Zolles, G., Bildl, W., Kulik, A., Heimrich, B., Chisaka, O., Jonas, P., Schulte, U., Fakler, B., and Klöcker, N. (2009) *Science* **323**, 1313-1319
63. Hoffman, L., Stein, R. a, Colbran, R. J., and McHaourab, H. S. (2011) *EMBO J* **30**, 1251-1262

64. Lu, W., Isozaki, K., Roche, K. W., and Nicoll, R. A. (2010) *Proc Natl Acad Sci U S A* **107**, 22266-22271
65. Kristensen, A. S., Jenkins, M. a, Banke, T. G., Schousboe, A., Makino, Y., Johnson, R. C., Huganir, R., and Traynelis, S. F. (2011) *Nat Neurosci* **14**, 727-735
66. Penzes, P. and Jones, K. a (2008) *Trends Neurosci* **31**, 419-427
67. Ciruela, F., Soloviev, M. M., Chan, W. Y., and McIlhinney, R. a (2000) *Mol Cell Neurosci* **15**, 36-50
68. Mao, L.-M., Liu, X.-Y., Zhang, G.-C., Chu, X.-P., Fibuch, E. E., Wang, L. S., Liu, Z., and Wang, J. Q. (2008) *Neuropharmacology* **55**, 403-408
69. Fischer von Mollard, G., Südhof, T. C., and Jahn, R. (1991) *Nature* **349**, 79-81
70. Zhen, M. and Jin, Y. (1999) *Nature* **401**, 371-375
71. Hallam, S. J., Goncharov, A., McEwen, J., Baran, R., and Jin, Y. (2002) *Nat Neurosci* **5**, 1137-1146
72. Yang, X., Kovalenko, O. V., Tang, W., Claas, C., Stipp, C. S., and Hemler, M. E. (2004) *J Cell Biol* **167**, 1231-1240
73. Van Itallie, C. M., Gambling, T. M., Carson, J. L., and Anderson, J. M. (2005) *J Cell Sci* **118**, 1427-1436
74. Cayouette, S. and Boulay, G. (2007) *Cell calcium* **42**, 225-232
75. Greaves, J. and Chamberlain, L. H. (2011) *Trends Biochem Sci* **36**, 245-253

76. El-Husseini, a E., Craven, S. E., Chetkovich, D. M., Firestein, B. L., Schnell, E., Aoki, C., and Brecht, D. S. (2000) *J Cell Biol* **148**, 159-172
77. Fang, C., Deng, L., Keller, C. a, Fukata, M., Fukata, Y., Chen, G., and Lüscher, B. (2006) *J Neurosci* **26**, 12758-12768
78. Fernández-Hernando, C., Fukata, M., Bernatchez, P. N., Fukata, Y., Lin, M. I., Brecht, D. S., and Sessa, W. C. (2006) *J Cell Biol* **174**, 369-377
79. Huang, K., Sanders, S., Singaraja, R., Orban, P., Cijssouw, T., Arstikaitis, P., Yanai, A., Hayden, M. R., and El-Husseini, A. (2009) *FASEB J* **23**, 2605-2615
80. Greaves, J., Carmichael, J. A., and Chamberlain, L. H. (2011) *Mol Biol Cell* **22**, 1887-1895
81. Johnson, D. R., Bhatnagar, R. S., Knoll, L. J., and Gordon, J. I. (1994) *Annu Rev Biochem* **63**, 869-914
82. Zhang, F. L. and Casey, P. J. (1996) *Annu Rev Biochem* **65**, 241-269
83. Iwanaga, T., Tsutsumi, R., Noritake, J., Fukata, Y., and Fukata, M. (2009) *Prog Lipid Res* **48**, 117-127
84. Greaves, J., Prescott, G. R., Fukata, Y., Fukata, M., Salaun, C., and Chamberlain, L. H. (2009) *Mol Biol Cell* **20**, 1845-1854
85. Greaves, J., Salaun, C., Fukata, Y., Fukata, M., and Chamberlain, L. H. (2008) *J Biol Chem* **283**, 25014-25026

86. Yanai, A., Huang, K., Kang, R., Singaraja, R. R., Arstikaitis, P., Gan, L., Orban, P. C., Mullard, A., Cowan, C. M., Raymond, L. a, Drisdell, R. C., Green, W. N., Ravikumar, B., Rubinsztein, D. C., El-Husseini, A., and Hayden, M. R. (2006) *Nat Neurosci* **9**, 824-831
87. Masuda, K., Itoh, H., Sakihama, T., Akiyama, C., Takahashi, K., Fukuda, R., Yokomizo, T., Shimizu, T., Kodama, T., and Hamakubo, T. (2003) *J Biol Chem* **278**, 24552-24562
88. Saitoh, R., Ohtomo, T., Yamada, Y., Kamada, N., Nezu, J.-I., Kimura, N., Funahashi, S.-I., Furugaki, K., Yoshino, T., Kawase, Y., Kato, A., Ueda, O., Jishage, K.-I., Suzuki, M., Fukuda, R., Arai, M., Iwanari, H., Takahashi, K., Sakihama, T., Ohizumi, I., Kodama, T., Tsuchiya, M., and Hamakubo, T. (2007) *J Immunol Methods* **322**, 104-117
89. Yoshida, T., Inoue, R., Morii, T., Takahashi, N., Yamamoto, S., Hara, Y., Tominaga, M., Shimizu, S., Sato, Y., and Mori, Y. (2006) *Nat Chem Biol* **2**, 596-607
90. Mansilla, F., Birkenkamp-Demtroder, K., Kruhøffer, M., Sørensen, F. B., Andersen, C. L., Laiho, P., Aaltonen, L. a, Verspaget, H. W., and Orntoft, T. F. (2007) *Br J Cancer* **96**, 1896-1903
91. Yamamoto, Y., Chochi, Y., Matsuyama, H., Eguchi, S., Kawauchi, S., Furuya, T., Oga, A., Kang, J. J., Naito, K., and Sasaki, K. (2007) *Oncology* **72**, 132-138

Figure Legends

Figure 1. The domain structure and phylogenetic tree of mammalian DHHC proteins (A)

DHHC proteins contain the conserved Cys-rich DHHC (Asp-His-His-Cys) domain and four or six transmembrane domains. Some subfamilies have unique motif/domain, such as PDZ-binding motif (DHHC3). (B) Phylogenetic tree of mammalian DHHC protein family members. 23 DHHC proteins can be categorized into some subfamilies based on the homology of the catalytic DHHC domains. For example, DHHC2 and 15 belong to the same subfamily (in red) while DHHC3 and 7 form another subfamily (in blue). The discovery of this mammalian palmitoyl acyl transferase (PAT) family and the establishment of simple screening system using DHHC protein library have facilitated identification of palmitoyl substrate-enzyme pairs. Importantly, the same subfamily of DHHC proteins often shares substrates. For example, DHHC2/15 subfamily (in red) specifically palmitoylates PSD-95 and GAP-43. DHHC3/7 subfamily (in blue) palmitoylates most of palmitoyl-proteins, such as PSD-95, GAP-43, G α , GABA $_A$ R γ 2, and SNAP-25, DHHC9/18 subfamily (in purple) palmitoylates H-Ras, DHHC21 (in brown) palmitoylates Lck and eNOS and DHHC17 (in yellow) palmitoylates SNAP-25. Thus, a large DHHC protein family represents PATs.

Figure 2. Identification of 10 novel palmitoyl substrates through *in silico* proteomics. (A)

TARP γ 2, TARP γ 8, cornichon-2 (CNIH2), CaMKII α , neurochondrin (Ncdn), Syd-1, TRPM8, TRPC1, orexin receptor type2 and zyxin were palmitoylated by metabolic labeling assay with

[³H]palmitate. Each candidate was co-expressed with DHHC3 palmitoylating enzyme in HEK293 cells, followed by incubation with [³H]palmitic acid ([³H]Palm) for 4 hours. HEK293 cells were then lysed, and proteins were separated by SDS-PAGE and analyzed by fluorography and Western blotting with indicated antibodies. Arrowheads indicate the position of individual candidates. **(B)** Endogenous TARP γ 8, CaMKII α , Ncdn and Syd-1 were palmitoylated in cultured hippocampal neurons. Hydroxylamine (NH₂OH)-sensitive palmitoylated proteins were purified from neurons by the ABE method. The sample was analyzed by Western blotting with indicated antibodies. Tris, Tris treatment as a control of hydroxylamine.

Figure 3. DHHC1, 3, 7 and 10 palmitoylate Ncdn. **(A)** Palmitoylation of Ncdn was enhanced by DHHC1, 3, 7 and 10, while TARP γ 8, CaMKII α and Syd-1 were palmitoylated by DHHC3/7 subfamily. Individual 23 DHHC proteins were co-expressed with Ncdn-GFP, TARP γ 8, CaMKII α -GFP or GFP-Syd-1 in HEK293 cells and metabolically labeled with [³H]palmitic acid ([³H]palm) as Figure 2A. HEK293 cells were lysed, and proteins were separated and analyzed by fluorography. Arrows indicate the position of palmitoylated substrates. **(B)** Palmitoylation of Ncdn was increased by DHHC1/10 and DHHC3/7 subfamilies. To quantify the relative palmitoylation activity of each DHHC enzyme, the ratio of intensity of palmitoylated Ncdn to that of total Ncdn by Western blotting and CBB (not shown) was quantified. The fold of an average intensity of three independent experiments to the background intensity is indicated below each lane. DHHC1 and 10 belong to the same subfamily in green and DHHC3 and 7

belong to the other subfamily in blue.

Figure 4. Mutation of Cysteines 3 and/or 4 abolishes palmitoylation of Ncdn. (A) Palmitoyl cysteines of Ncdn predicated by CSS-Palm 2.0. Cys-3 and Cys-4 are the most potential cysteines for palmitoylation sites. The protein sequence of Ncdn was analyzed by CSS-Palm 2.0 and the position and the score of each potential cysteine were shown. The small bars at the bottom indicate the positions of cysteines with low potential (score <0.8). (B) Ncdn, as well as PSD-95 and CaMKII α , are suggested to be highly brain-enriched palmitoyl proteins. The X-axis indicates the score of brain enrichment calculated from BodyMap-Xs gene expression database. The cut-off point is 0.75. The Y-axis is the score of CSS-Palm 2.0. The cut-off point is 1.8. (C) Ncdn palmitoylation sites are Cys-3 and Cys-4. Either Cys-3 or Cys-4 or both Cys-3 and Cys-4 were mutated to serine (Ncdn C3S, Ncdn C4S or Ncdn C3,4S). Ncdn WT and mutants were co-expressed with DHHC1, 2, 3, 7, 10 or 14 in HEK293 cells and analyzed by metabolic labeling assay. The mutations on Cys-3 and Cys-4 abolished Ncdn palmitoylation. (D) DHHC10 physically interacts with Ncdn. Hisx6-Flag-DHHC2, 3 and 10 were expressed in HEK293 cells and the lysates were mixed with the membrane fraction from rat brain. Hisx6-Flag-DHHC proteins were tandem affinity-purified with Flag antibody agarose and subsequently Ni-NTA agarose. The purified samples (IAP) were analyzed by Western blotting with anti-Ncdn antibody. (E) DHHC1 and DHHC10 specifically palmitoylate Ncdn. Ncdn-GFP, G α_q -GFP and GluA2-Flag were co-expressed with DHHC1, 10, 3, 7, 2 and 20 in HEK293 cells and analyzed

by metabolic labeling assay. Arrow indicates the position of Ncdn. CBB, Coomassie brilliant blue staining. Black lines indicate the subfamily members. **(F)** Palmitoyl cysteines of Ncdn have to be located at the N-terminus. The N-terminal, or C-terminal, GFP tagged Ncdn was co-expressed with DHHC3 or 10 in HEK293 cells. Arrow indicates the position of Ncdn. **(G)** The N-terminal four-amino acids, MSCC (Met-Ser-Cys-Cys), are necessary and sufficient for palmitoylation by DHHC3 and 10. The N-terminal peptides of Ncdn were fused with GFP and co-expressed with DHHC3 or 10 in HEK293 cells. N3, Met-Ser-Cys; N4, Met-Ser-Cys-Cys; N5, Met-Ser-Cys-Cys-Asp. Arrow indicates the position of fusion proteins. White asterisks indicate bands due to the autopalmitylation of DHHC3 and 10.

Figure 5. DHHC1/10 subfamily is localized in dendritic shafts and dendritic spines.

Hippocampal neurons were transfected with **(A)** HA-DHHC1 and 10, **(B)** HA-DHHC3 and 7, **(C)** HA-DHHC2 and 15, and **(D)** HA-DHHC5 and 8, and doubly immunostained with anti-HA and anti-PSD-95 at 20 DIV. Some populations of DHHC1 and 10 proteins were localized in dendritic shafts and dendritic spines. DHHC3/7 was specifically localized at the Golgi apparatus. DHHC2/15 subfamily was localized in dendritic vesicles. DHHC5/8 subfamily was localized in dendritic surface membrane. Right bar, 10 μm ; Left bar, 5 μm .

Figure 6. Developmental change in expression and subcellular localization of Ncdn. **(A)** The antibody to Ncdn, N-rNcdn, specifically recognizes a single 75 kDa band in rat hippocampal

neuron lysate, rat cortical neuron lysate, rat brain P2 fraction lysate and mouse brain homogenate. (B) Expression of Ncdn increased between 7 and 14 DIV. In cultured cortical neurons, Ncdn expression was hardly detected at 3 DIV, began to be detected at 7 DIV and was the highest at 14 DIV, and declined but was higher at 21-28 DIV than 7 DIV. Importantly, this expression pattern of Ncdn in cultured neurons was very similar to that of mGluR5. Moesin was examined as an internal control. (C) Ncdn is enriched in cytoplasmic (S3) and postsynaptic density (PSD1 and 2) fractions. Subcellular distribution of Ncdn was examined by biochemically fractionating the brain homogenate. Ncdn protein was fractionated into both cytoplasmic (S3) and membrane fractions (P2), and was further fractionated into both TritonX-100-soluble (Sol1) and -insoluble (PSD1 and PSD2) fractions from P2-derived synaptosome fraction. Fractionation was successful, as a postsynaptic marker protein, PSD-95, was fractionated exclusively into PSD fractions. Ncdn was enriched in S3 and PSD fractions.

Figure 7. Ncdn is specifically localized in dendrites. (A) Knockdown effects of miR-Ncdn were verified by co-expression of Ncdn-HA with individual miRNA constructs in HEK293 cells. miR-Ncdn803 was more efficient than miR-Ncdn1270. Moesin was examined as an internal control. GFP was examined to see the expression of miRNAs. (B) Ncdn antibody (N-rNcdn) specifically recognizes endogenous Ncdn in neurons. Cortical neurons were knocked-down by microRNA (miRNA; miR-Ncdn) and immunostained with anti-N-rNcdn antibody (red). White arrow indicates knocked-down neuron visualized with GFP (green). Bar, 10 μ m. (C and D) Ncdn

is localized in dendrites but not in the axon, and partially localized in dendritic spines (white arrows). Hippocampal neurons were co-immunostained with anti-Ncdn and either anti-MAP2 (dendritic marker), anti-pan-axonal neurofilament (NF) (axonal marker), anti-PSD-95 (postsynaptic marker) or anti-synaptophysin (Syp, presynaptic marker) antibody. Upper bar, 10 μm ; Lower bar, 5 μm . Arrows indicate the co-localization of Ncdn with PSD-95 (upper), and the apposition to synaptophysin (lower). **(E)** DHHC10 and Ncdn are co-localized in dendritic spines (white arrows). Hippocampal neurons were transfected with HA-DHHC3 or HA-DHHC10 and immunostained with anti-HA (red), anti-Ncdn (green) and anti-PSD-95 (blue) antibodies (23 DIV). (Right panels) upper, HA; middle, Ncdn; lower, merge. Left bar, 10 μm ; Right bar, 5 μm . **(F)** Ncdn WT-GFP is redistributed at a perinuclear region by DHHC10 (white arrow), but not by DHHC3. Ncdn WT-GFP or Ncdn C3,4S-GFP was co-expressed with GST, DHHC3 or DHHC10 in COS7 cells and live-imaged. Bar, 20 μm .

Figure 8. Localization of Ncdn in dendritic membrane structures depends on its palmitoylation. **(A)** No significant difference is observed in hippocampal neurons expressing Ncdn WT and palmitoylation-deficient Ncdn (Ncdn C3,4S). Ncdn WT-GFP or Ncdn C3,4S-GFP was transfected into hippocampal neurons and immunostained with GFP at 22 DIV. Bar, 10 μm **(B)** Ncdn WT-GFP is distinctly localized in the somato-dendritic membrane structures, while GFP and Ncdn C3,4S-GFP were localized in the cytoplasm in dendrites. Hippocampal neurons were transfected with GFP, Ncdn WT-GFP or Ncdn C3,4S-GFP at 8 DIV, pre-treated with 0.1%

TritonX-100 before fixation, and immunostained with anti-GFP antibody. White arrows indicate the localization of Ncdn WT-GFP in the dendritic membrane structure. Bar, 10 μ m.

Figure 9. Suppression of DHHC1 expression reduces Ncdn in dendrites. (A) Knockdown effects of miR-DHHC1 and mi-DHHC10 were verified by co-expression of HA-DHHC1 or HA-DHHC10 with individual miRNA constructs in HEK293 cells. miR-DHHC1_532 and miR-DHHC10_171 were more efficient than miR-DHHC1_911 and miR-DHHC10_312. (B and C) Hippocampal neurons were transfected with miRNA-LacZ (miR-LacZ, control miRNA.), miR-DHHC1_532, miR-DHHC3_735, or miR-DHHC10_171. Neurons were immunostained with anti-Ncdn and anti-MAP2 at around 20 DIV. Knocked-down neurons were visualized by GFP. When DHHC1 was knocked-down, the intensity of Ncdn in dendrites significantly decreased. In contrast, knockdown of DHHC3 and DHHC10 had no effects on dendritic localization of Ncdn. The average intensity of Ncdn in dendrites (30-50 μ m from the cell body) was quantified. The average intensity of Ncdn was normalized to that of MAP2. $n = 32$ neurons from four independent experiments. $**P < 0.01$. Upper bar, 10 μ m; Lower bar, 5 μ m.

Table 1. Human disorders associated with palmitoyl acyl transferases (PATs)

DHHC protein	Disorders associated with PATs	References
DHHC2	Colorectal cancer	(11)
DHHC8	Schizophrenia	(12-14)
DHHC9	X-linked mental retardation	(16)
	Colorectal cancer	(90)
DHHC11	Bladder cancer	(91)
DHHC15	X-linked mental retardation	(15)
DHHC17/HIP14	Huntington disease	(17, 86)

Table 2. Gene list of the substrate candidates

Name	Acc. No.	Sp	Forward primer	Reverse primer	Tag	Provider
TARP γ 2	NM_053351	Rt			HA	David Brecht (Johnson & Johnson, NJ)
TARP γ 8	NM_133190	Ms				David Brecht (Johnson & Johnson, NJ)
Homer 1C	AB007688	Rt			GFP	Akihiko Kato (Eli Lilly, IN)
Kalirin7	AF230644	Rt			GFP	Xin-Ming Ma (Univ. of Connecticut Health Science Center, CT)
KIF5C560	NM_001107730	Rt			YFP	Gary Banker (Oregon Health Science University, OR)
TRPC1	NM_003304	Hu			Flag	Yasuo Mori (Kyoto University)
OX2R	NM_198962	Ms			GFP	Akihiro Yamanaka (NIPS, Japan)
Paxillin	NM_002859	Hu			GFP	Kozo Kaibuchi (Nagoya University)
Zyxin	NM_001010972	Hu			GFP	Kozo Kaibuchi (Nagoya University)
TRPM8	NM_134252	Ms	5'-GCTAGAATTCGCCACCATGT CCTTCGAGGGAGCCAGGCT-3'	5'-GCTAGAATTCTTACTTGTGCG TCGTCATCCTTGTAGTCCTGA TGTTATTAGCAATCTCTT-3'	Flag	TRPM8: Ardem Patapoutia (The Scripps, CA)
CaMKII α	NM_012920	Rt	5'-GCTAGAATTCGCCACCATGG CTACCATCACCTGCACCCG-3'	5'-GCTAGCGGCCGCCATGGGG CAGGACGGAGGGCGCCCCAGA TCTGT-3'	GFP	mGFP-CaMKII α : Bayer Ulli (UC Denver, CO)

Liprin- α 2	AF034799	Hu	5'- GCTAGAATTCGCCACCATGATG TGTGAAGTGATGCCACGATTA A-3'	5'-GCTAGAATTCTCAACATGAG TATGTGCGAACAG-3'		HA-liprin: Davis Bredt (Johnson & Johnson, NJ)
Neurochondrin	NM_001025132	Rt	5'-GCTAGAATTCGCCACCATGT CGTGTTGTGACCTGGC-3'	5'-GCTAGCGGCCGCGGGGCTC TGACAGGCACTGCTCCA-3'	GFP HA	(RT-PCR)
Cornichon-2	NM_001025132	Rt	5'-GCTAGAATTCGCCACCATGG CGTTCACCTTCGCAGCATT-3'	5'-GCTAGAATTCGAAGCTCACC AACGTATAAACCA-3'	GFP	(RT-PCR)
Rab3A	NM_013018	Rt	5'-GCTAGAATTCACCATGGCCT CAGCCACAGACTCTCG-3'	5'-GCTAGAATTCTCAGCAGGCG CAATCCTGATGAG-3'	GFP	(RT-PCR)
Syd-1	NM_001191876	Rt	5'-GCTAGAATTCACCATGGCCG AGCCGCTGCTCAGGAA-3'	5'-GCTAGAATTCTCAGAGGCAC ACATTGATCTGCTT-3'	GFP	(RT-PCR)
Par3 (1-843)	NM_031235	Rt	5'-GCTAGAATTCACCATGAAAG TGACCGTGTGCTTCGG-3'	5'-GCTAGAATTCTCCATCGTTG GGGACTTGACGA-3'	GFP	(RT-PCR)

Acc. No., GenBank/EMBL/DDBJ accession number; Sp, Species; Rt, Rat; Ms, Mouse; Hu, Human; Forward primer and reverse primer are the primer sets used for PCR or RT-PCR.

Table 3. Selected palmitoyl candidates in this study

Category	Name	Highest CSS-Palm score	Position	Sequence	Brain enrich. score	Metabolic labeling	ABE method
Postsynapse	TARP γ 2	1.913	121	GGL C IAA	0.85	+	NT
	TARP γ 8	2.461	144	GGV C VAA	0.75	+	+
	Cornichon-2	2.266	62	RIC C LLR	0.90	+	NT
	CaMKII α	3.765	6	TIT C TRF	0.88	+	+
	Kalirin7	2.297	1422	LLT C CEE	ND	-	NT
	Homer 1C	2.687	365	LLE C S**	ND	-	NT
	Neurochondrin	13.016	3	*M S CCDL	0.82	+	+
Presynapse	Rab3A	2.313	220	DCAC C ***	0.91	-	NT
	Syd-1	3.078	734	INV C L**	ND	+	+
	Liprin- α 2	4.783	3	*MM C EVM	0.89	-	NT
Motor	KIF5C	2.183	7	PAE C SIK	ND	-	NT
TRP channel	TRPM8	4.234	1032	FK C CKE	0.75	+	NT
	TRPC1	2.547	752	KVM C CLV	0.83	+	NT
GPCR	Orexin receptor type2	3.5	381	AF S CCLG	0.83	+	NT
Focal adhesion	Paxillin	2.278	557	KL F C***	ND	-	NT
	Zyxin	1.952	412	C F TCHQC	ND	+	NT
Tight junction	Par3	3.061	6	VT V CFGR	ND	-	NT

“Category” indicates where substrate candidates were categorized based on their localization and functions. “Name” indicates candidate protein name. “Highest CSS-Palm score,” “position” and “Sequence” indicate the highest score in the protein given by CSS-Palm 2.0, the position of the corresponding cysteine (in red), and the sequence around the cysteine. “Brain enrich. score”

indicates brain enrichment score, where “ND” means no data. “Metabolic labeling” indicates the result of metabolic labeling assay with [³H]palmitate, where “+” means that the candidate was palmitoylated while “-“ means not palmitoylated. “ABE method” indicates the result of ABE method, where “+” means that the endogenous protein was palmitoylated; “NT” , not tested.

Table 4. Top 10 palmitoyl candidates enriched in brain

Rank	UniProt Acc. No.	CSS-Palm Score	Description	#Unigene	Brain Enrichment
1	P06837	16.84	Growth associated protein 43	Mm.1222	0.95
2	P54830	14.47	Protein tyrosine phosphatase, non-receptor type 5	Mm.4654	0.97
3	Q3URJ8	13.75	Na ⁺ /K ⁺ transporting ATPase interacting 3	Mm.317473	0.77
4	P60761	13.44	Neurogranin	Mm.335065	0.92
5	Q3URA8	13.16	Predicted gene, ENSMUSG00000072769	Mm.131865	0.89
6	Q8BVS1	13.09	Centaurin, alpha 1	Mm.297819	0.77
7	Q9Z0E0	13.02	Neurochondrin (Ncdn)	Mm.456184	0.82
8	Q9D6H4	12.66	Coiled-coil domain containing 13	Mm.450959	1.00
9	P60202	12.59	Proteolipid protein (myelin) 1	Mm.1268	0.98
10	Q5HZI5	12.13	Protocadherin 17	Mm.153643	0.75

The table shows a ranking of potential palmitoyl substrates according to the score by CSS-Palm

2.0. Neurochondrin is the 7th highest palmitoyl candidate among proteins with high brain

enrichment score (>0.75). “UniProt Acc. No.” indicates the accession number of UniProt

database, where the protein sequences were extracted. “CSS-Palm score” indicates the highest

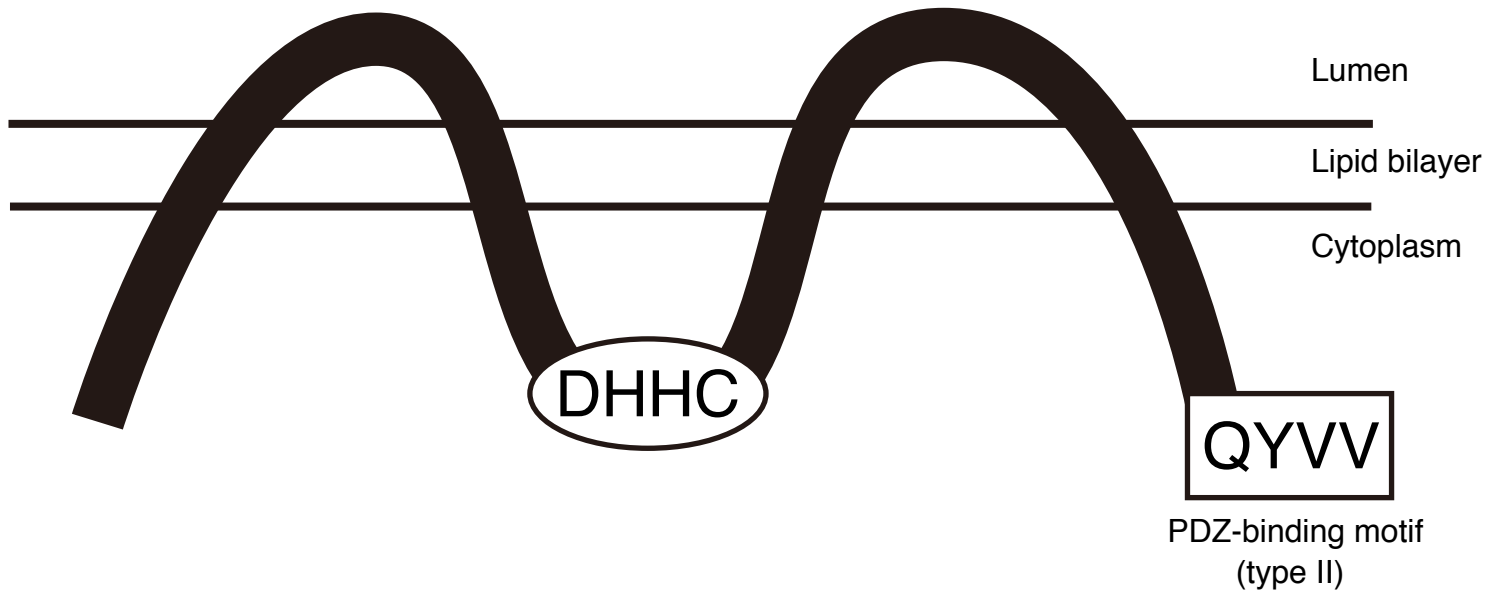
score that each candidate has. “#Unigene” indicates the accession number used in BodyMap-Xs.

“Brain enrichment” indicates the calculated score (Maximum 1.00- Minimum 0.00) for brain

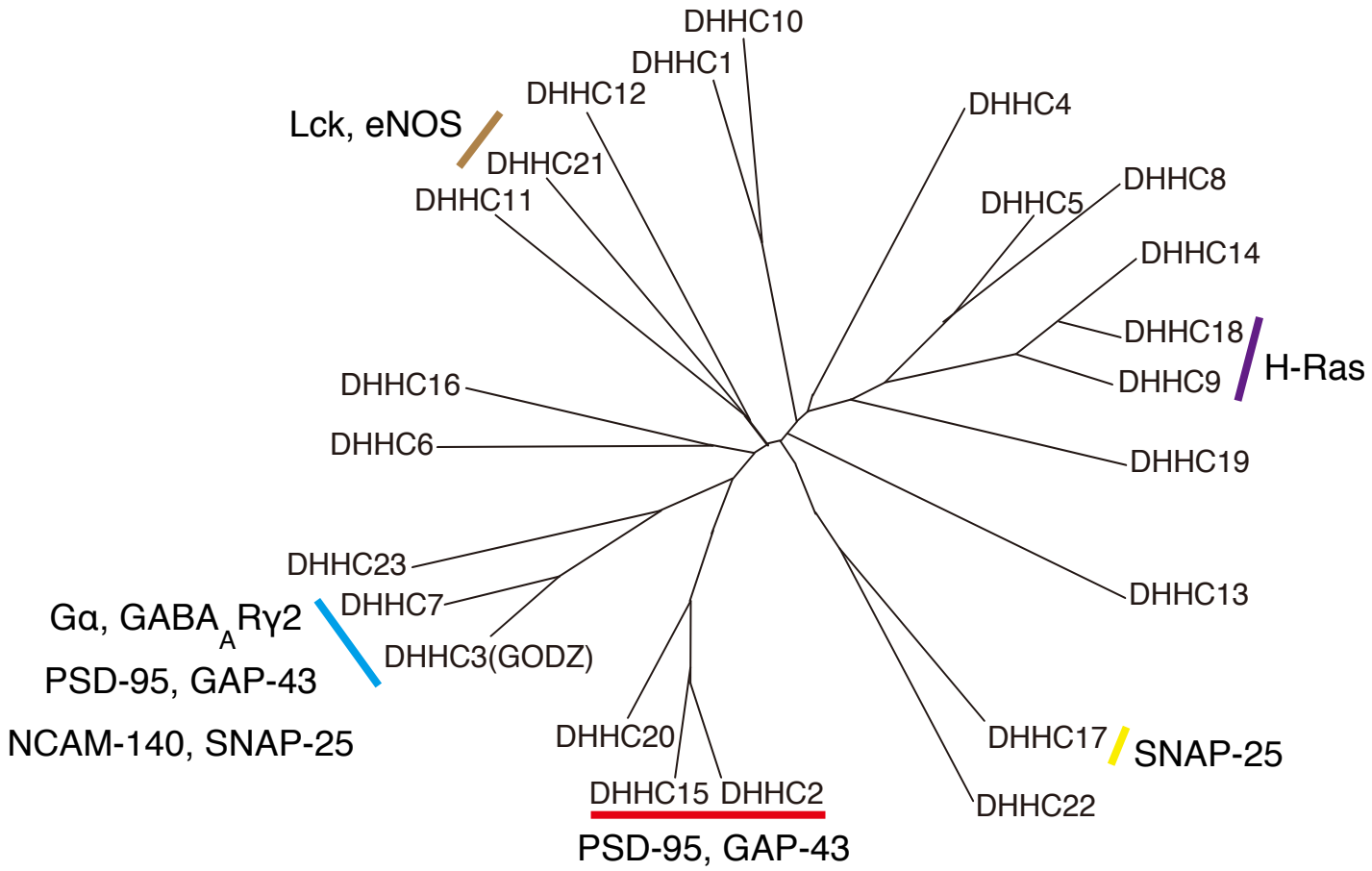
enrichment based on BodyMap-Xs data. Protein with brain enrichment score >0.7 was assumed as brain enriched proteins.

A

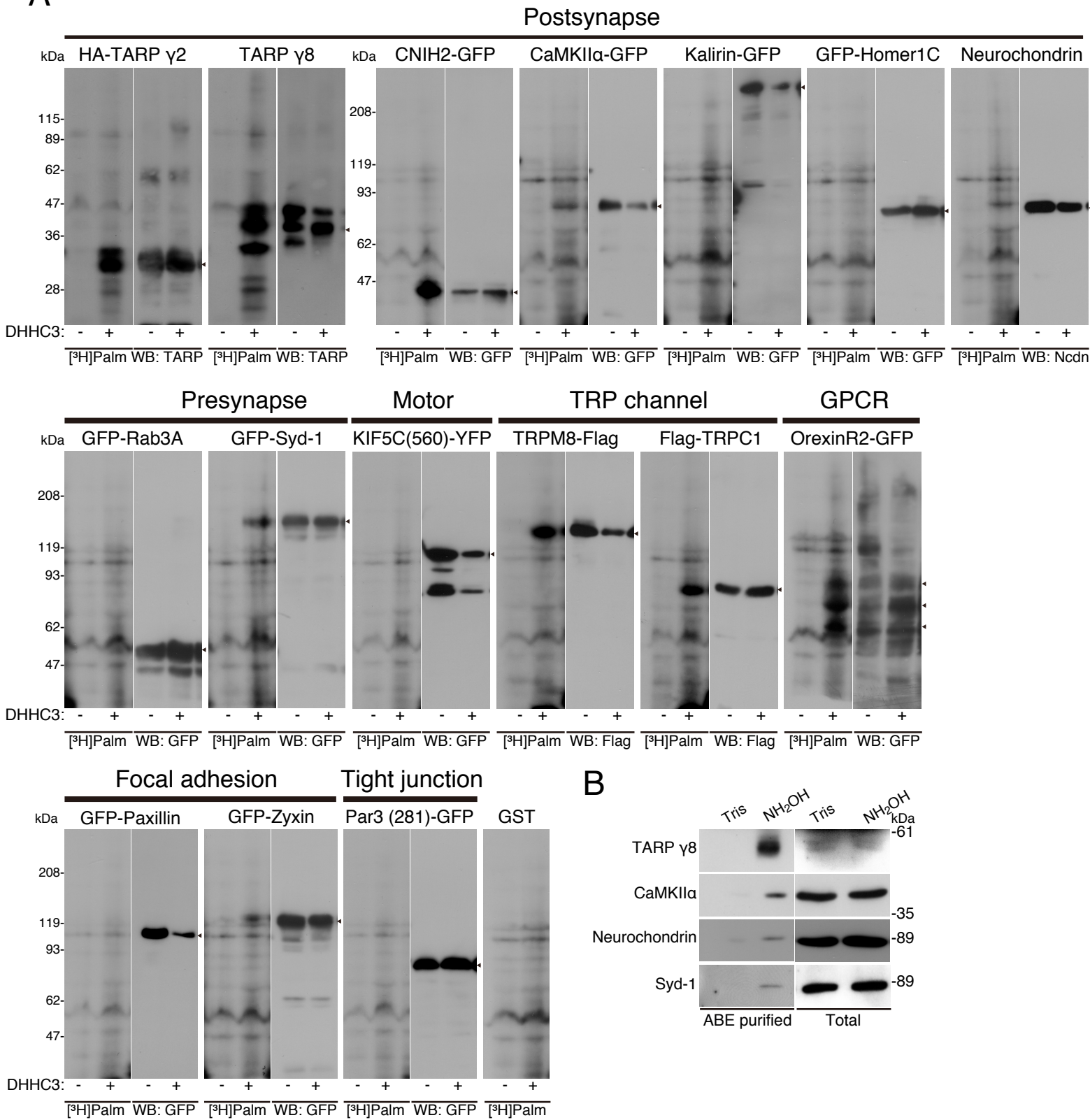
DHHC3



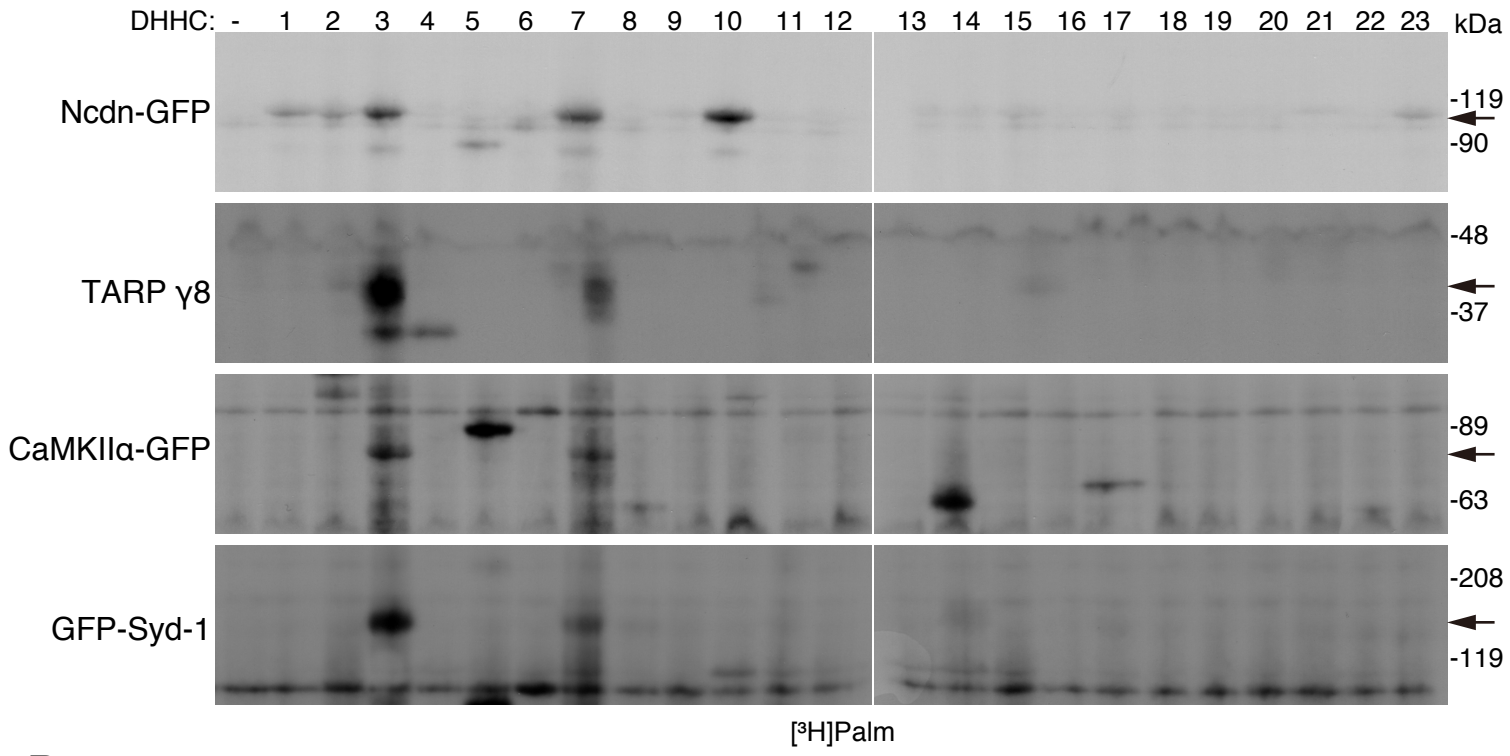
B



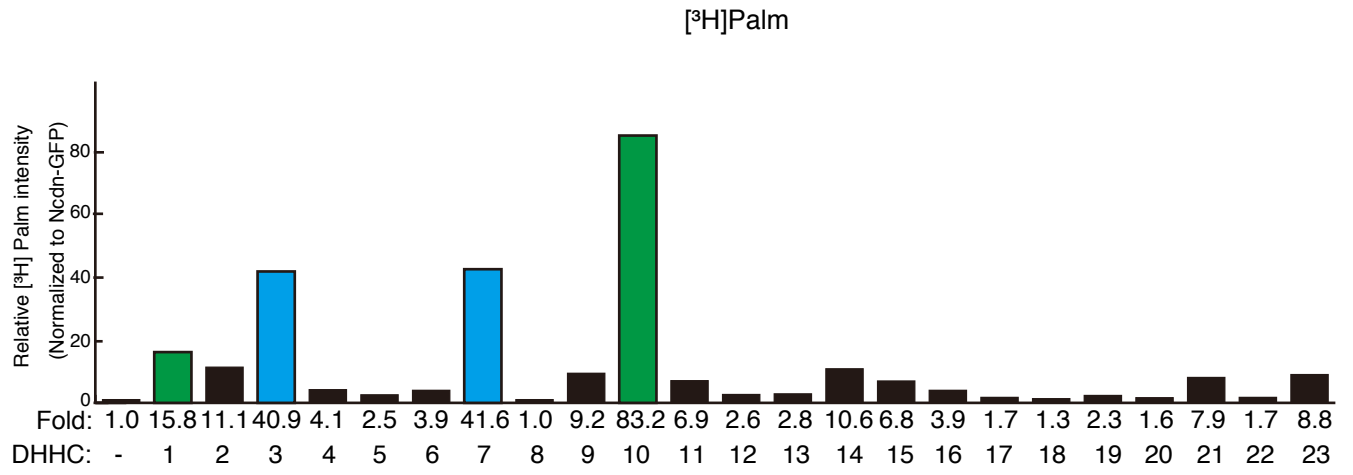
A

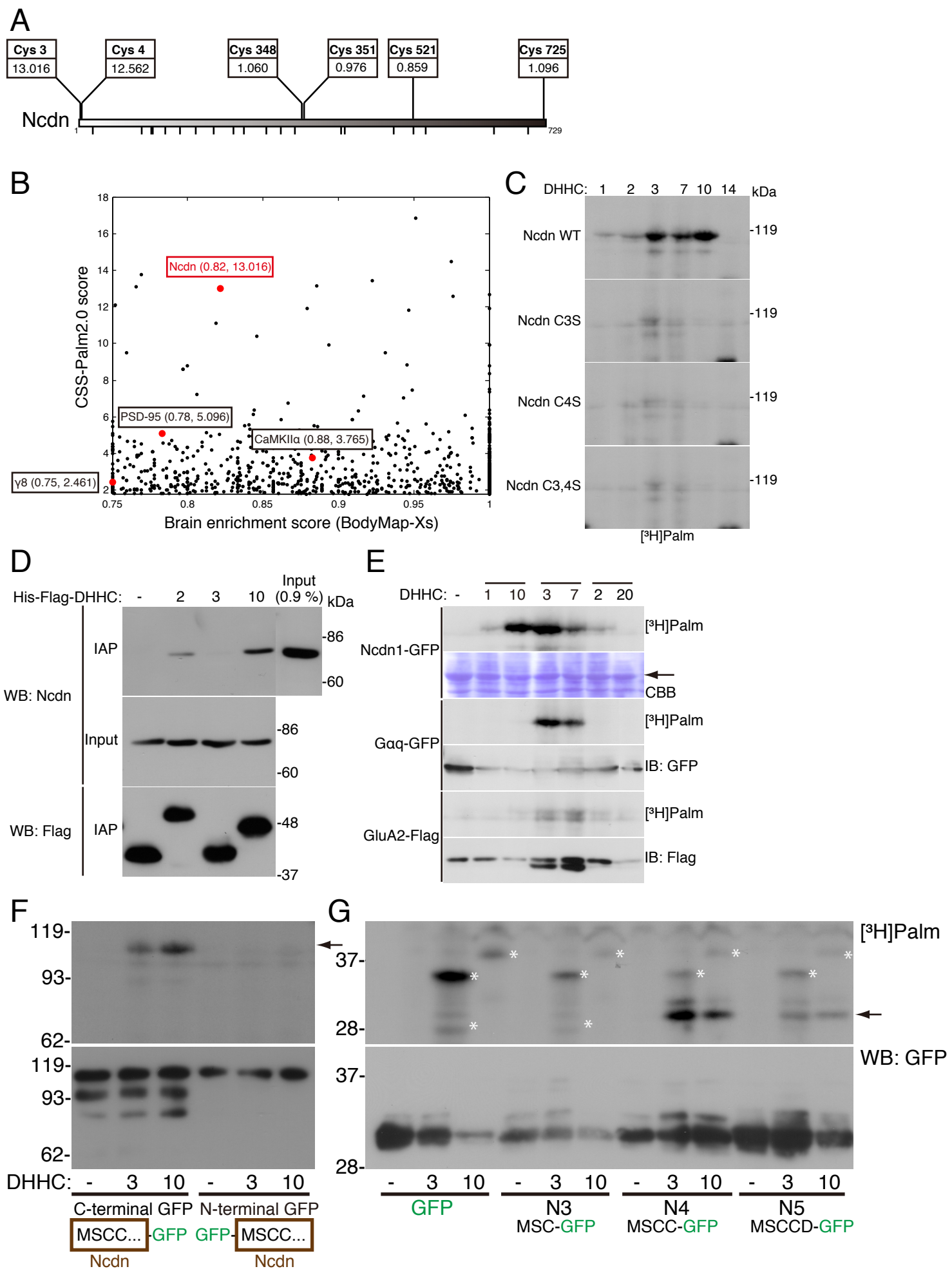


A

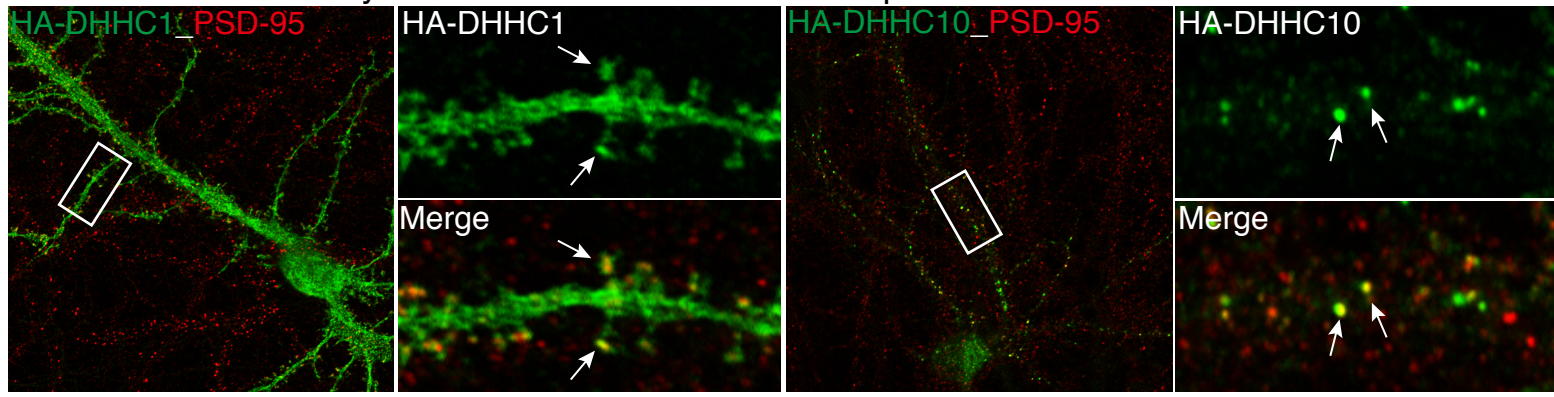


B

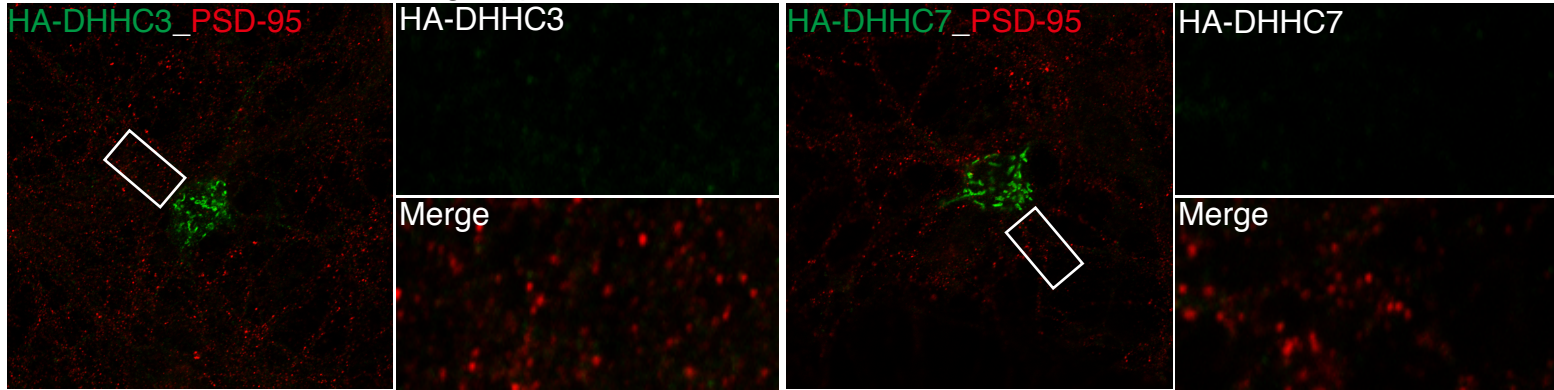




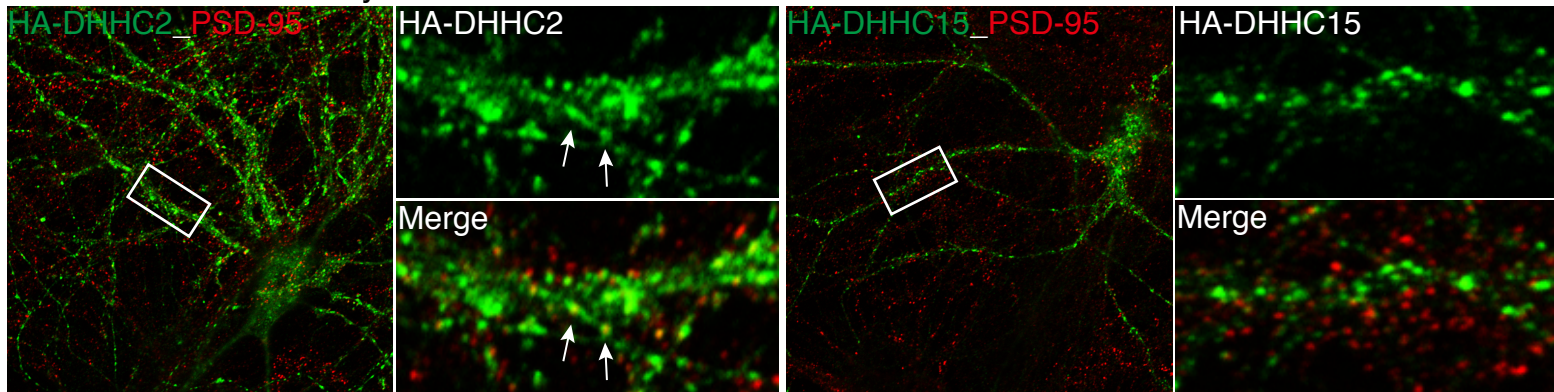
A DHHC1/10 subfamily - Dendritic shafts and dendritic spines



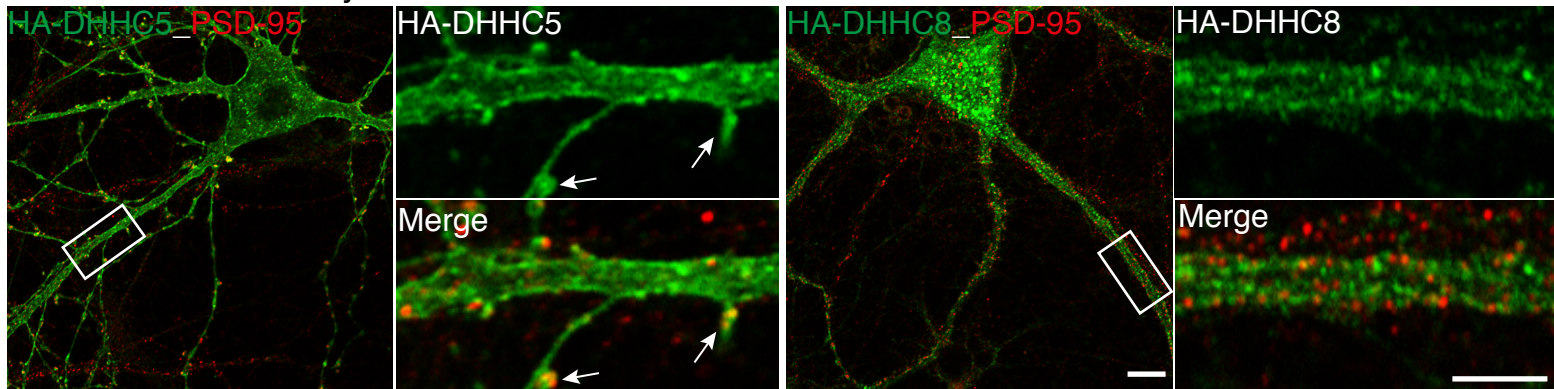
B DHHC3/7 subfamily - Golgi apparatus

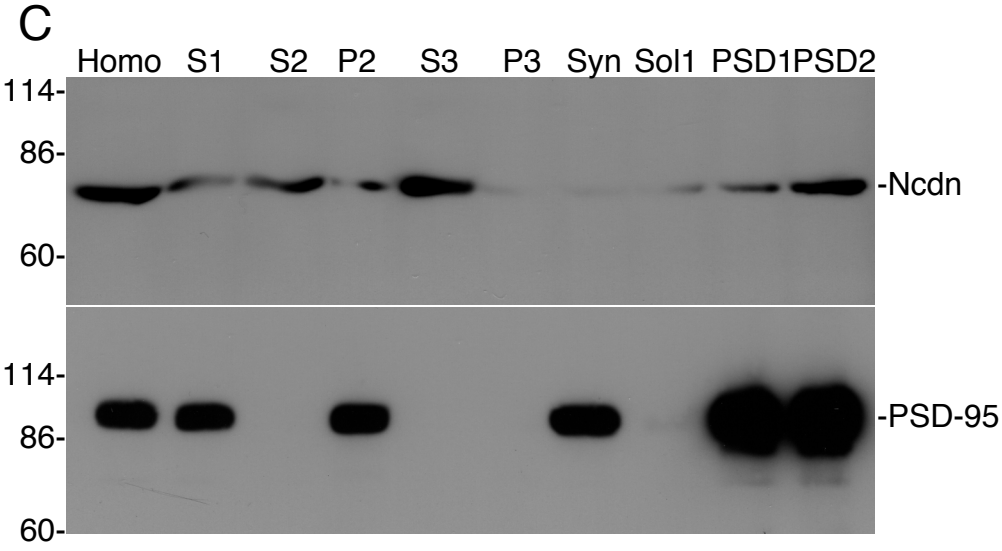
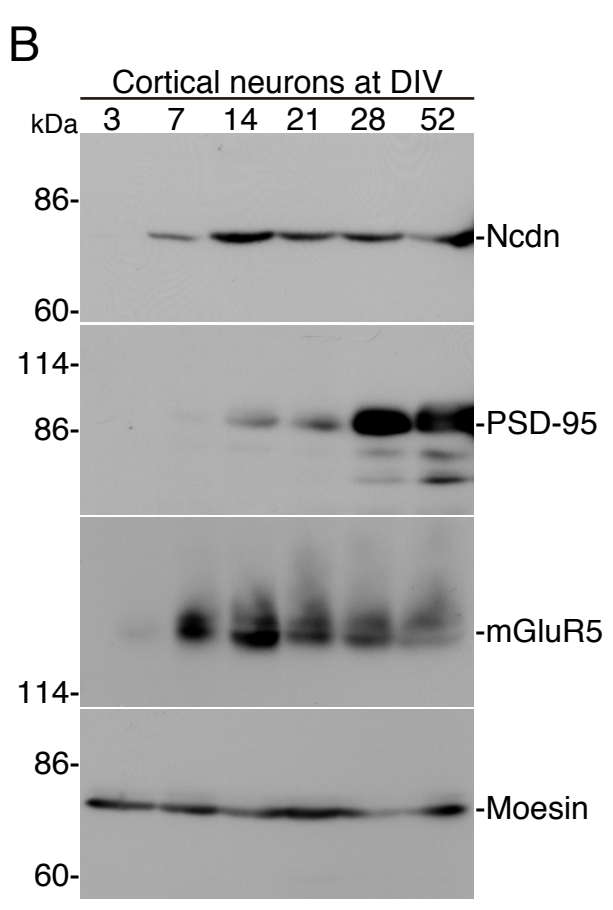
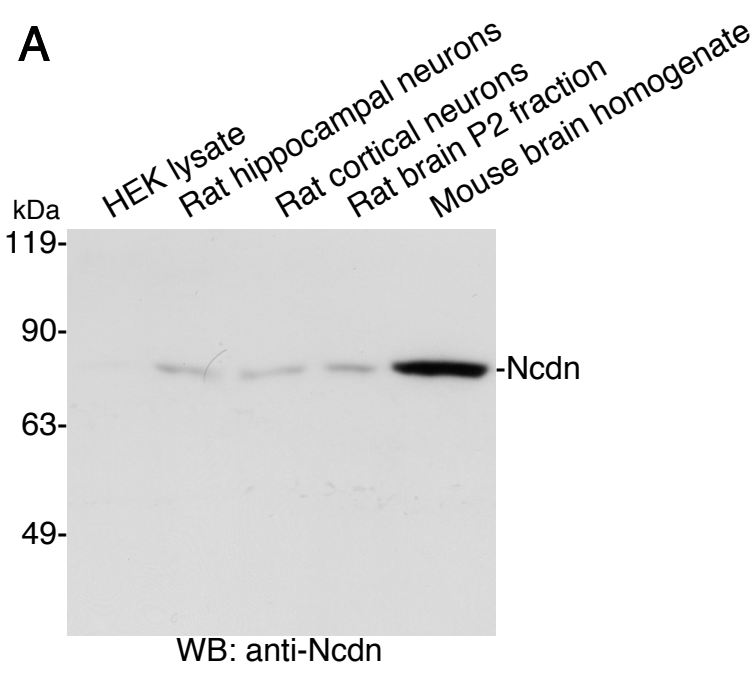


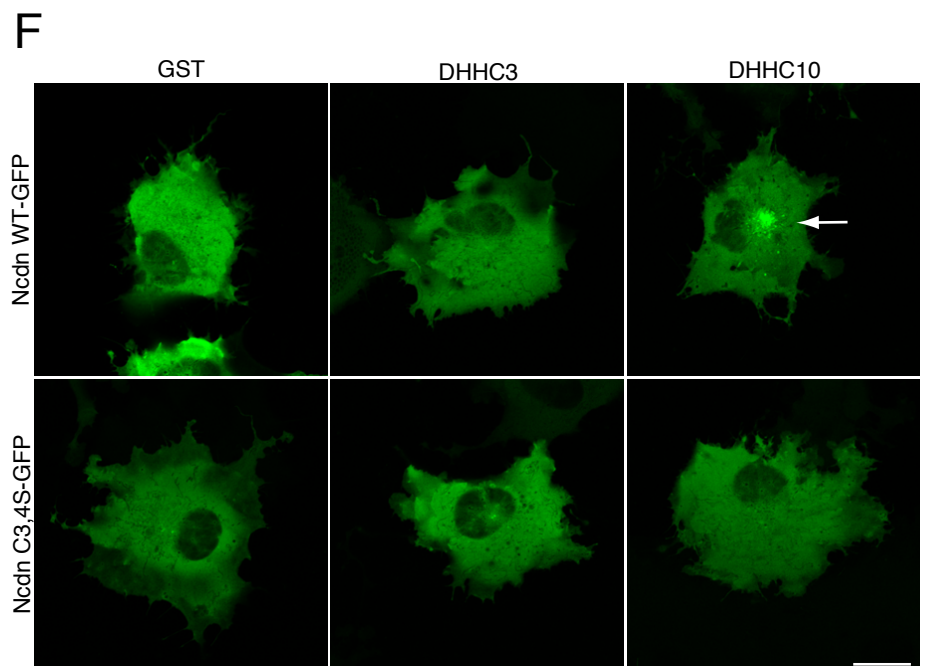
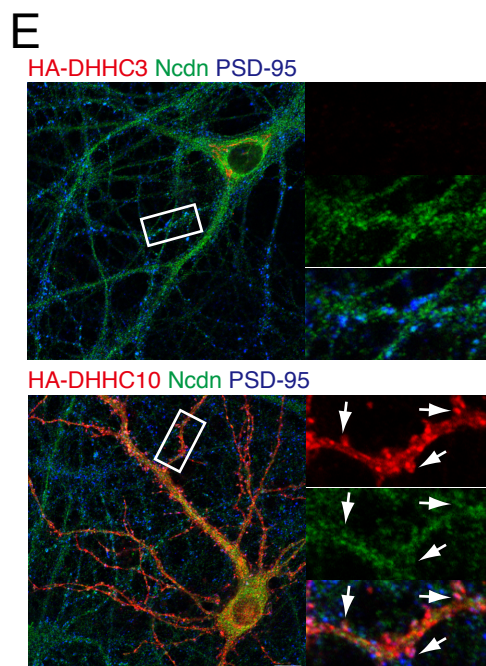
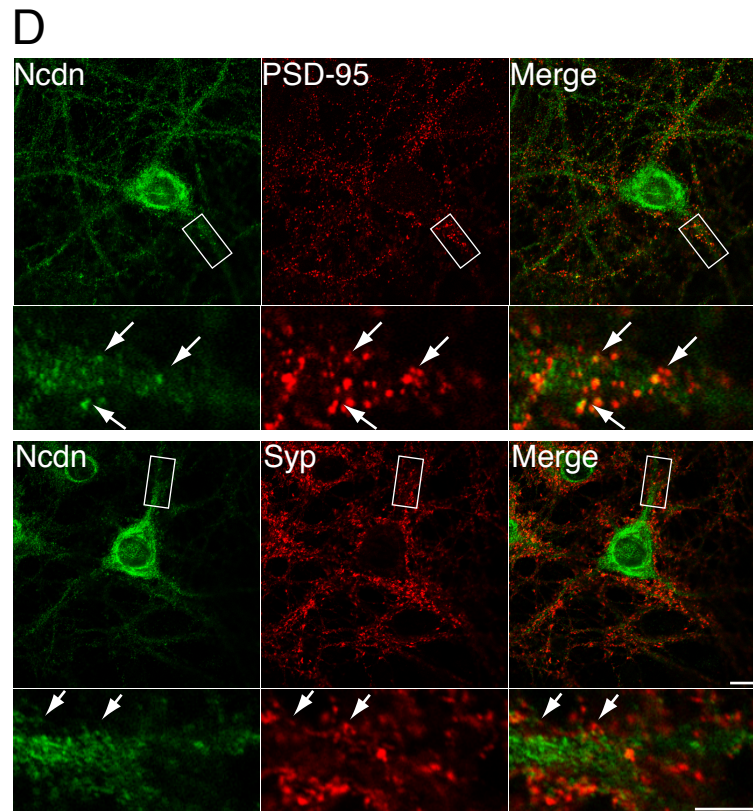
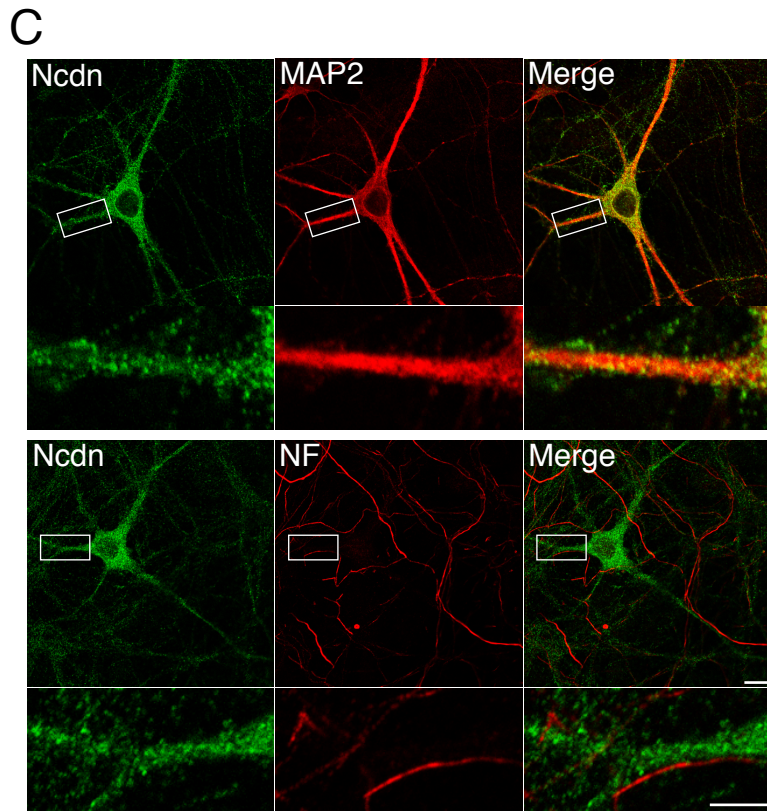
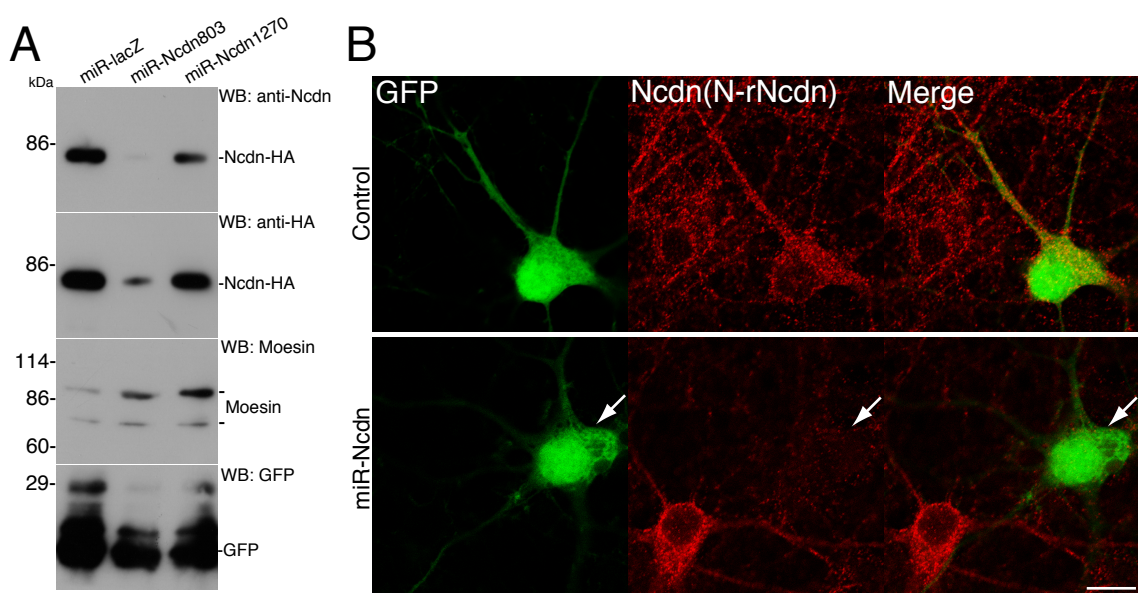
C DHHC2/15 subfamily - Dendritic vesicles



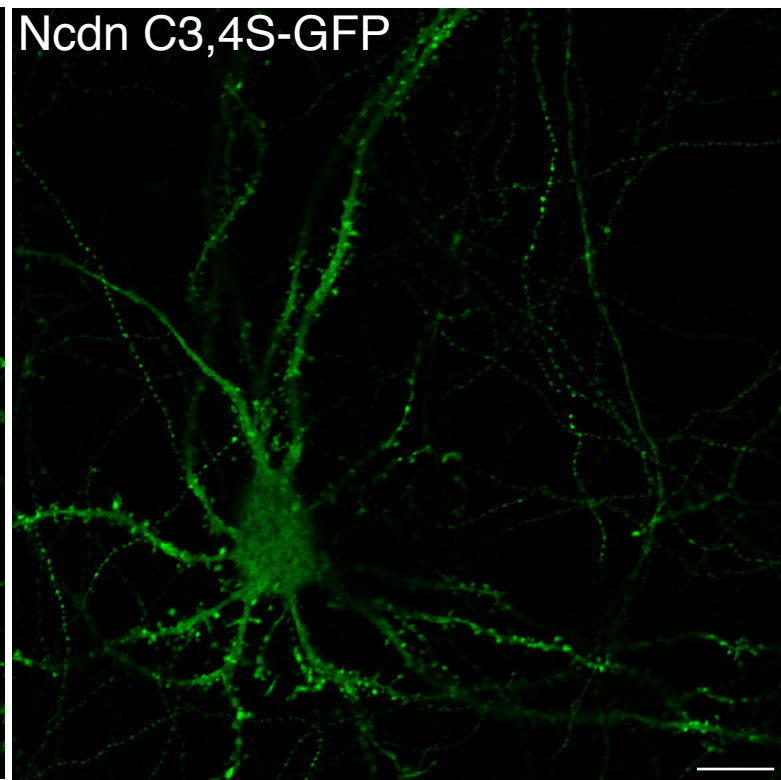
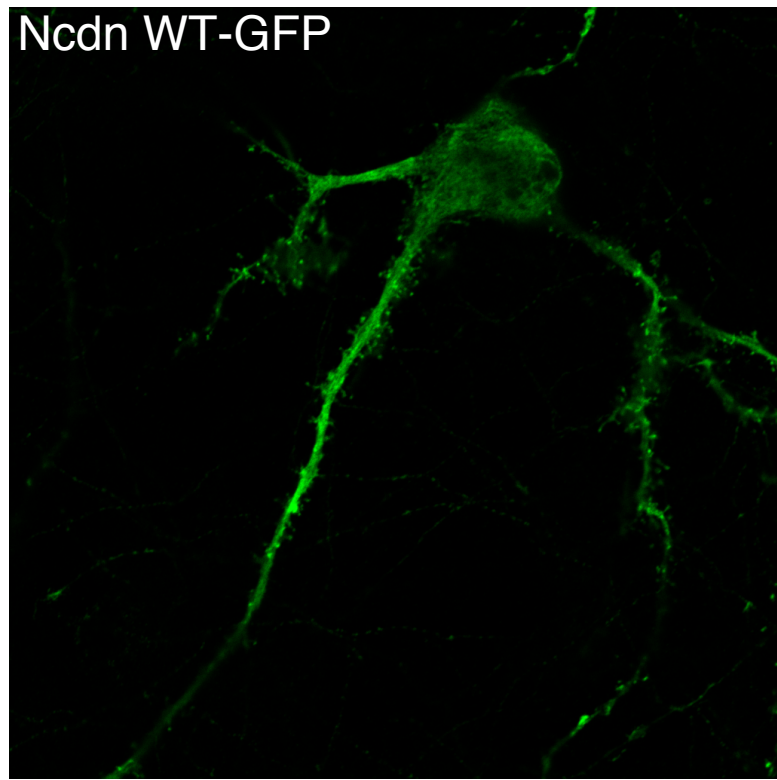
D DHHC5/8 subfamily - Dendritic surface







A



B

